

Nonparametric Bayesian Multi-Treatment Mixture Cure Survival Model with Application in Pediatric Oncology

Peter Chang¹, John Kairalla¹, Arkaprava Roy¹

¹*University of Florida, Gainesville, USA,*

October 29, 2025

Abstract

Heterogeneous treatment effect estimation is critical in oncology, particularly in multi-arm trials with overlapping therapeutic components and long-term survivors, as often seen in pediatric cancer studies. These structural characteristics pose a central challenge to estimating treatment effects in precision medicine for pediatric oncology. We propose a novel covariate-dependent nonparametric Bayesian multi-treatment cure survival model that jointly accounts for common structures among treatments and cure fractions. Through latent link functions, our model leverages sharing among treatments through a flexible modeling approach, enabling individualized survival inference. We adopt a Bayesian route for inference and implement an efficient MCMC algorithm for approximating the posterior. Simulation studies demonstrate the method's robustness and superiority in various specification scenarios. Finally, application to the AALL0434 trial reveals clinically meaningful differences and some novel insights in survival across methotrexate-based regimens and their associations with different covariates, underscoring its practical utility for learning treatment effects in real-world pediatric oncology data.

Keywords: Bayesian inference; Children Oncology; Cure fraction; Multi-treatment regime; Neural network; Survival probability; Treatment effect.

1 Introduction

Estimating individualized treatment effects plays a crucial role in personalized medicine. In oncology trials, survival-related outcomes are the primary endpoints (Powers et al., 2018; Xu et al., 2024; Hu et al., 2021). Particularly, in chemotherapy trials, patient outcomes can differ markedly between treatment regimens. For instance, our motivating application, the Children’s Oncology Group (COG) AALL0434 trial for pediatric acute lymphoblastic leukemia, compares multiple methotrexate-based regimens, all of which share common therapeutic components with a largely common therapeutic backbone (Dunsmore et al., 2020). Failing to account for shared characteristics among treatment arms may result in inefficient treatment effect estimation. Estimating heterogeneous treatment effects in such settings poses two main challenges, where we need to 1) account for overlapping treatment mechanisms and 2) model survival data with a substantial proportion of patients achieving long-term remission and thus are effectively cured, as shown in pediatric oncology and other long-term survival settings.

These challenges highlight the need for a flexible survival model to estimate heterogeneous treatment effects while accommodating cure fractions and leveraging shared structure across treatment arms. Ignoring cured patients may bias survival estimates, while treating treatment arms independently can lead to inefficient inference, particularly in multi-arm trials with overlapping components.

Mixture cure models offer a principled approach to account for long-term survivors by decomposing the population into cured and susceptible subgroups (Boag, 1949; Berkson and Gage, 1952). Estimation of mixture cure models has been explored in both frequentist and Bayesian settings. In the frequentist framework, the expectation-maximization (EM)

algorithm is commonly used for mixture models to help estimate the latent cure status (Kuk and Chen, 1992; Zhang and Peng, 2007; Peng and Taylor, 2011), while Bayesian approaches rely on Markov chain Monte Carlo (MCMC) methods with data augmentation (Kuo and Peng, 2000; De la Cruz et al., 2022; Pan et al., 2024). However, traditional data-augmentation-based MCMC can be difficult to implement when jointly modeling cure status and heterogeneous treatment effects.

We propose a Bayesian mixture cure model that jointly estimates cure and survival probabilities across treatment groups with shared therapeutic characteristics. The model is built on a mixture framework for survival times, incorporating shared components to enable partial pooling of information across related treatments. Subject-specific mixture weights and cure probabilities are modeled using latent link functions, enabling flexible individual heterogeneity while borrowing information across arms with common components, addressing the limitation of T-learning type models as pointed out by Künzel et al. (2019). We additionally consider two variations of this structure: one with linear latent links and the other modeled by a neural network (NN) structure. To address the computational challenges of high-dimensional posterior sampling, we adopt a gradient-based MCMC approach based on the marginal likelihood function, circumventing the need for full data augmentation. For treatment effect inference, we utilize a linear projection-based estimator following Semenova and Chernozhukov (2021); Cui et al. (2023), and then apply a thresholding procedure for variable importance quantification as proposed in Chang and Roy (2025), combining it with a data partitioning mechanism.

Our method makes several contributions towards applying survival methodologies in the context of multi-arm clinical trials. We develop a nonparametric Bayesian mixture model

that is amenable to estimating survival outcome-based treatment effect quantification. Our model also incorporates a cure component, which allows us to account for long-term survival settings. Then, by incorporating both linear and NN links, we increase our model's flexibility to account for hidden relationships between the outcome and other covariates. Finally, we propose a novel data-partition and marginal best linear projection-based inference scheme to identify important variables and interpret treatment effect estimation. Applying our method to pediatric oncology data, we demonstrate its ability to uncover treatment effect heterogeneity in the presence of shared treatment structure and patients who are cure.

The remainder of this article is organized as follows. The subsequent section introduces the COG trial AALL0434 to which we will apply our proposed method. Section 3 introduces our covariate-dependent non-parametric mixture-cure model. In Section 4, we discuss the Bayesian inference scheme, detailing the prior specification, likelihood computation, posterior computation steps, and our inference scheme. Subsequently, in Section 5, we analyze and compare the effectiveness of our proposed method against another competing approach under various cure and data generation settings. Finally, we apply our proposed method to the AALL0434 trial data in Section 6, and finally, Section 7 is dedicated to discussing the overall conclusion and potential extensions.

2 AALL0434 dataset

Data analyzed in this study comes from ALL0434, a Phase III randomized study conducted by the Children's Oncology Group (Dunsmore et al., 2020) to evaluate treatment strategies for children and young adults with newly diagnosed T-cell acute lymphoblastic leukemia (T-ALL) or T-cell lymphoblastic lymphoma (T-LL). The study enrolled 1,895 patients between

2007 and 2014, collecting data on demographics, clinical characteristics, treatment regimens, and outcomes. Patients were stratified into risk groups based on central nervous system (CNS) involvement, minimal residual disease (MRD) after induction therapy, white blood cell (WBC) count and age at diagnosis, and other clinical features, such as mediastinal masses and extramedullary disease.

The trial evaluated the efficacy of adding nelarabine to the augmented Berlin-Frankfurt-Münster (ABFM) chemotherapy regimen, compared high-dose methotrexate (HDMTX) to escalating-dose methotrexate with pegaspargase (C-MTX) during interim maintenance, and explored the omission of cranial radiation therapy (CRT) in lower-risk patients. The primary outcome was five-year disease-free survival (DFS), with secondary outcomes including overall survival and CNS relapse rates. The addition of nelarabine significantly improved DFS among T-ALL patients, while the C-MTX regimen outperformed HDMTX in DFS during interim maintenance.

Our data contains 1146 patients with different patient demographics such as age at diagnosis and also predictors related to the study such as treatment arm, risk group, central nervous system (CNS) status, white blood cell (WBC) count, and indication of testicular disease. This data contains two survival outcomes: disease free survival and overall survival with their respective censoring indicators.

To ensure comparability across treatment groups, we restrict our analysis to patients who were randomly assigned to treatment arms. As noted in Winter et al. (2018), patients with CNS status 3 or testicular involvement were non-randomly assigned to HDMTX-containing arms. Excluding these cases yields a final cohort of 1,022 patients.

To better understand patient characteristics and outcomes by treatment arm, we analyze

Table 1: Demographics Table of the AALL0434 Clinical Trial Data Set Stratified by Treatment Arm. Continuous variables presented as Mean (SD), while categorical variables presented as n(%). We present the 5-year disease-free and overall survival as outcomes.

Variable	All	C-MTX	C-MTX/nelarabine	HD-MTX	HD-MTX/nelarabine
N	1022	370 (36.2%)	145 (14.2%)	362 (35.4%)	145 (14.2%)
Age (years)	9.9 (5.3)	9.7 (5.3)	10.5 (5.8)	9.5 (5.1)	10.9 (5.5)
WBC Count (μ L)	147.9 (180.3)	146.1 (177.2)	153.1 (182.8)	144.2 (168.1)	156.7 (213.9)
Sex					
Female	248 (24.3%)	86 (23.2%)	37 (25.5%)	88 (24.3%)	37 (25.5%)
Male	774 (75.7%)	284 (76.8%)	108 (74.5%)	274 (75.7%)	108 (74.5%)
Risk Group					
High risk T-ALL	210 (20.5%)	55 (14.9%)	51 (35.2%)	52 (14.4%)	52 (35.9%)
Intermediate risk T-ALL	703 (68.8%)	261 (70.5%)	94 (64.8%)	255 (70.4%)	93 (64.1%)
Low risk T-ALL	109 (10.7%)	54 (14.6%)	0 (0%)	55 (15.2%)	0 (0%)
CNS Status					
1	810 (79.3%)	286 (77.3%)	113 (77.9%)	295 (81.5%)	116 (80%)
2	212 (20.7%)	84 (22.7%)	32 (22.1%)	67 (18.5%)	29 (20%)
5 year Disease Free Survival	806 (78.9%)	303 (81.9%)	114 (78.6%)	279 (77.1%)	110 (75.9%)
5 year Overall Survival	831 (81.3%)	312 (84.3%)	115 (79.3%)	292 (80.7%)	112 (77.2%)

key demographic, clinical, and risk factors across the four treatment groups: C-MTX, C-MTX with nelarabine, HD-MTX, and HD-MTX with nelarabine. We provide a demographics table of the study population in Table 1. When looking at the survival outcomes, 78.9%

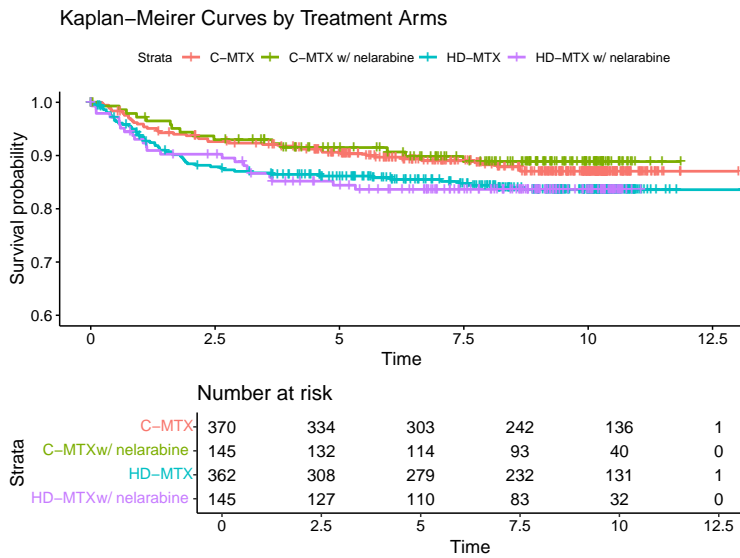


Figure 1: Disease free survival (DFS) Kaplan-Meier curve estimation of the treatment arms from the AALL0434 Clinical Trial.

of the cohort remained disease-free after five years with an overall survival rate of 81.3%.

The highest disease free survival rate was seen in the C-MTX group, whereas HDMTX with nelarabine was the lowest. As an exploratory analysis, we plot the Kaplan-Meier curves for each treatment arm in Figure 1. Additionally, we also plot the Kaplan-Meier curves stratifying by key categorical covariates in Figures S2-S6. We see that the survival probability is the highest for patients using C-MTX with nelarabine, while those using HDMTX was the lowest. We see that all tails of the curves have a plateau, indicating that a cure model may be more appropriate to use (Othus et al., 2012).

3 Mixed-cure survival model

In standard survival analysis, it is often assumed that all individuals are susceptible to the event of interest and will eventually experience it, given sufficient follow-up. However, in many clinical contexts, a subset of patients may be considered cured and no longer at risk of the event. Following Peng and Dear (2000) and Li et al. (2007), we characterize the overall survival probability as a mixture model. The mixture cure model, proposed by Farewell (1982), is composed of two parts that encompasses two groups of patients: those that cured and those who are susceptible.

Let T denote the random variable representing the time until an event occurs. We define $B = I(T < \infty)$ as indicator of susceptibility, where $B = 1$ denotes a susceptible individual and $B = 0$ denotes a cured individual. Let t be the survival time for the i -th patient. Then, our proposed model for the survival function, when treated under the g -th treatment, is

$$S_g(t \mid \mathbf{x}_i) = c_g(\mathbf{x}_i) + \{1 - c_g(\mathbf{x}_i)\}S_{g,u}(t \mid \mathbf{z}_i) \quad (1)$$

where $c_g(\mathbf{x}_i) = P(B_i = 0 \mid \mathbf{x}_i)$ represents the probability that an individual i belongs to the

group of non-susceptible subjects that will never experience the event, and $S_{g,u}(t \mid \mathbf{z}_i) = P(T > t \mid \mathbf{Z} = \mathbf{z}_i, B = 1)$ is the survival function of the susceptible. Our covariate matrices \mathbf{X} and \mathbf{Z} reflect covariates that can affect the two groups, respectively. In this paper, we consider $\mathbf{z}_i = \mathbf{x}_i$ i.e. \mathbf{Z} is identical to \mathbf{X} (Sy and Taylor, 2000; Lee et al., 2024; Cai et al., 2012) such that the same covariates affect both the cured and susceptible patients. We characterize $c_g(\mathbf{x}_i)$ as,

$$c_g(\mathbf{x}_i) = \frac{\exp(f_g^{(\text{cure})}(\mathbf{x}_i))}{1 + \exp(f_g^{(\text{cure})}(\mathbf{x}_i))} = \frac{1}{1 + \exp(-f_g^{(\text{cure})}(\mathbf{x}_i))}, \quad (2)$$

where $f_g^{(\text{cure})}(\cdot)$ can be any unrestricted function of the covariates.

Next, we discuss our model for the survival probability, $S_{g,u}(t \mid \mathbf{x}_i)$, of the susceptible subjects. Here, we consider a covariate-dependent group-specific mixture of log-normals and let $S_{g,u}(t \mid \mathbf{x}_i, \boldsymbol{\mu}, \boldsymbol{\sigma}) = \sum_{m=1}^M \pi_{i,m,g} Q_m(t)$, where $Q_m(t) = P_{(\mu_m, \sigma_m)}(T > t)$, under a univariate Log-normal distribution with parameters μ_m and σ_m . The weights $\pi_{i,m,g}$ are modeled using a softmax output function

$$\pi_{i,m,g} = \frac{\gamma_{m,g} \exp(f_m^{(\text{surv})}(\mathbf{x}_i))}{\sum_{j=1}^M \gamma_{j,g} \exp(f_m^{(\text{surv})}(\mathbf{x}_i))}, \quad (3)$$

where the parameter $\boldsymbol{\Gamma} = ((\gamma_{m,g}))_{1 \leq m \leq M, 1 \leq g \leq G}$ is a $M \times G$ binary matrix. This matrix plays a crucial role in our proposed model, controlling the set of mixture components to be used in the survival function of the susceptible. In the following subsections, we propose two possible choices for $f_g^{(\text{cure})}$'s and $f_m^{(\text{surv})}$'s. We call them the latent link functions. Motivated by our application, we next further discuss two forms for our functions: a linear form and a nonlinear neural network form.

3.1 Linear Latent Link

We first consider a simpler case with linear links and let $f_g^{(\text{cure})}(\mathbf{x}_i) = \mathbf{x}_i^T \boldsymbol{\lambda}_g = \lambda_{g,0} + \sum_{p=1}^P x_{i,p} \lambda_{g,p}$ and for the m -th weight, $f_m^{(\text{surv})}(\mathbf{x}_i) = \mathbf{x}_i^T \boldsymbol{\beta}_m = \beta_{m,0} + \sum_{p=1}^P x_{i,p} \beta_{m,p}$, where the first element of \mathbf{x}_i is 1 to include intercepts λ_0 and $\beta_{m,0}$ for both functions, respectively. Each $\lambda_{g,p}$ measures the increase in susceptibility under each group g and predictor p for a given patient. Likewise, each $\beta_{m,p}$ quantifies how predictor p influences the relative weighting of survival mixture component m . We present a schematic of our model in Figure 2.

Because all covariates behave linearly, this specification is straightforward to estimate and yields coefficients that are easy to interpret. However, the additive structure cannot capture any nonlinear or higher-order interactions among covariates. In these scenarios, the linear link will mis-specify those patterns. This limitation motivates our move to a shared, nonlinear basis expansion via a single-hidden-layer neural network, which can flexibly approximate such complex effects.

3.2 Neural Network Link with Shared Neurons

Now, we propose to model link functions nonparametrically, allowing greater flexibility in relating the covariates with corresponding survival probabilities. This also offers greater flexibility while analyzing real-world data. Specifically, we use the NN architecture and let $f_g^{(\text{cure})}(\mathbf{x}_i) = \lambda_{g,0} + \sum_{k=1}^K \lambda_{g,k} \psi(\mathbf{x}_i^T \boldsymbol{\theta}_k)$ and $f_m^{(\text{surv})}(\mathbf{x}_i) = \beta_{m,0} + \sum_{k=1}^K \beta_{m,k} \psi(\mathbf{x}_i^T \boldsymbol{\theta}_k)$, where the activation function is set as the hyperbolic tangent function $\psi(a) = \frac{e^{2a}-1}{e^{2a}+1}$.

Thus, each latent function is characterized as a linear combination of smooth, sigmoidal basis functions that can capture complex, nonlinear covariate effects. From a functional-approximation perspective, the linear combination of these bases allows the network to ap-

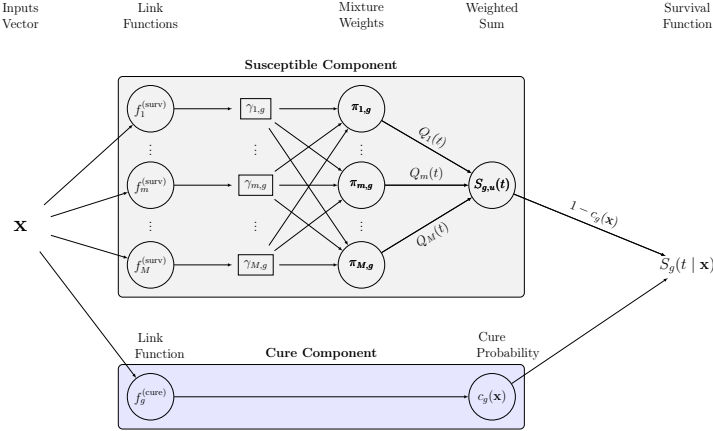


Figure 2: Schematic of the proposed mixture cure model with group effect. Covariates \mathbf{x}_i are fed into two parallel linear link functions, corresponding to the susceptible and cure probabilities. For the susceptible component, the $\gamma_{m,g}$'s are binary and control the inclusion of the weights into the sum.

proximate any continuous function on a compact domain, with K being the number of neurons. Our choice of K is further explained in Section 4.5, where we discuss a cross-validation method balancing model complexity and performance. Early results from Hornik et al. (1989); Cybenko (1989) establish that a single hidden layer with a sufficient number of neurons possesses universal approximation properties, allowing our NN link functions to reflect non-linear effects of the covariates (Anastassiou, 2011; Xu and Reich, 2023). In our mixture-cure setting, sharing both the neurons and activation functions across all the latent links $f_m^{(\text{surv})}(\mathbf{x})$'s and $f_g^{(\text{cure})}(\mathbf{x})$ with function-specific weights ensures complex dependencies are learned jointly.

Section 4 discusses our Bayesian inference scheme detailing the prior specification, likelihood computation, and additional settings such as the specification of K and M with other hyperparameters.

4 Bayesian Inference

We pursue a Bayesian approach to carry out the inference of the proposed cure mixture model. In our model, $\{\boldsymbol{\Gamma}, \boldsymbol{\mu}, \boldsymbol{\Lambda}, \boldsymbol{\beta}\}$ is the complete set of parameters in the linear link case and $\{\boldsymbol{\Gamma}, \boldsymbol{\mu}, \boldsymbol{\Lambda}, \boldsymbol{\beta}, \boldsymbol{\theta}\}$ is the complete parameter space in the NN link case. Here, the group-specific cure coefficients are stacked into $\boldsymbol{\Lambda} = \{\boldsymbol{\lambda}_0, \boldsymbol{\lambda}_1, \dots, \boldsymbol{\lambda}_G\}$ which is $G \times (P+1)$ dimensional for linear case and $G \times (K+1)$ dimensional for non-linear case. Similarly, we can form $\boldsymbol{\beta} = \{\boldsymbol{\beta}_0, \boldsymbol{\beta}_1, \dots, \boldsymbol{\beta}_P\}$ which $M \times (P+1)$ dimensional for linear case and $M \times (K+1)$ dimensional in case of the NN link. Finally the total number of mixture components $M \in \mathbb{R}$ and also the number of neurons $K \in \mathbb{R}$. Although M and K are both unknown, we first specify the priors assuming a given value of M and K . In Section 4.4, our specification procedure for M is discussed following an empirical Bayes-type strategy. Then, a predictive likelihood-based approach for selecting K is discussed in Section 4.5. In the following subsections, we discuss the priors of our parameters, the likelihood function of our model, and the posterior sampling steps we used to obtain posterior samples.

4.1 Prior Specification

To proceed with our Bayesian analysis, we put prior distributions on the parameters. We assume independent priors for $\boldsymbol{\Gamma}, \boldsymbol{\mu}, \boldsymbol{\Lambda}, \boldsymbol{\beta}$. They are described below in detail.

1. The basis inclusion indicators ($\boldsymbol{\Gamma}$): The indicators are independent and follow Bernoulli distribution as $\gamma_{k,g} \sim \text{Bernoulli}(p_g)$ where $p_g \sim \text{Beta}(c, d)$.
2. The mixture centers, cure coefficients, weight coefficients ($\boldsymbol{\mu}, \boldsymbol{\Lambda}, \boldsymbol{\beta}$): We put a multivariate normal distribution as the prior $\mu_m \sim \text{Normal}(0, \sigma_\mu^2)$, $\lambda_p \sim \text{Normal}(0, \sigma_\lambda^2)$,

$\beta_{p,k} \sim \text{Normal}(0, \sigma_\beta^2)$. We also propose that $\sigma_\mu^2, \sigma_\lambda^2, \sigma_\beta^2$ have an Inverse Gamma prior such that $\sigma_\mu^2, \sigma_\lambda^2, \sigma_\beta^2 \sim IG(a, b)$ with a pre-specified a, b .

4.2 Likelihood Function

For survival models, the likelihood function is derived based on the observed survival or censoring time t_i and the event indicator δ_i . For any subjects censored ($\delta_i = 1$), then the likelihood function is

$$p(\mathbf{t} \mid \boldsymbol{\mu}, \boldsymbol{\sigma}, \boldsymbol{\beta}, \boldsymbol{\Gamma}, \boldsymbol{\Lambda}, \mathbf{x}) = \prod_{i=1}^N \prod_{g=1}^G c_g(\mathbf{x}_i) + \{1 - c_g(\mathbf{x}_i)\} \sum_m \pi_{i,m,g} \left(1 - \Phi_m \left(\frac{\log(t_i) - \mu_m}{\sigma_m} \right) \right).$$

For any subjects uncensored ($\delta_i = 0$), the likelihood function is

$$p(\mathbf{t} \mid \boldsymbol{\mu}, \boldsymbol{\sigma}, \boldsymbol{\beta}, \boldsymbol{\Gamma}, \boldsymbol{\Lambda}, \mathbf{x}) = \prod_{i=1}^N \prod_{g=1}^G \{1 - c_g(\mathbf{x}_i)\} \sum_m \pi_{i,m,g} \frac{1}{t_i \sqrt{2\pi\sigma_m^2}} \exp \left\{ -\frac{(\log(t_i) - \mu_m)^2}{2\sigma_m^2} \right\}$$

Then the likelihood function with both contributions for all subjects becomes

$$\begin{aligned} p(\mathbf{t} \mid \boldsymbol{\mu}, \boldsymbol{\sigma}, \boldsymbol{\beta}, \boldsymbol{\Gamma}, \boldsymbol{\Lambda}, \mathbf{x}) &= \prod_{i=1}^N \prod_{g=1}^G S(t_i \mid \boldsymbol{\lambda}_g, \mathbf{x}_i, \boldsymbol{\mu}, \boldsymbol{\sigma}) \mathbb{1}(\delta_i = 1) + f(t_i \mid \boldsymbol{\lambda}_g, \mathbf{x}_i, \boldsymbol{\mu}, \boldsymbol{\sigma}) \mathbb{1}(\delta_i = 0) \\ &= \prod_{i=1}^N \prod_{g=1}^G \left[c_g(\mathbf{x}_i) + \{1 - c_g(\mathbf{x}_i)\} \sum_m \pi_{i,m,g} \left(1 - \Phi_m \left(\frac{\log(t_i) - \mu_m}{\sigma_m} \right) \right) \right]^{\delta_i} \\ &\quad \times \left[\{1 - c_g(\mathbf{x}_i)\} \sum_m \pi_{i,m,g} \frac{1}{t_i \sqrt{2\pi\sigma_m^2}} \exp \left\{ -\frac{(\log(t_i) - \mu_m)^2}{2\sigma_m^2} \right\} \right]^{1-\delta_i} \end{aligned}$$

We derive the expressions for the likelihood in the supplementary material in Section S1.

4.3 Posterior sampling

We use the Langevin Monte Carlo (LMC) sampling by utilizing the gradients of the posterior log-likelihood for each parameter except for the binary indicators in Γ . The binary indicators are updated element-wise using full-conditional Gibbs updates. The required gradients are provided in Supplementary Section S2, and additional sampling details are in Section S3.

4.4 Specification of M

To determine the number of components in the mixture model, we take a data-driven approach. We first apply the `Mclust` function, used for model-based clustering, classification, and density estimation based on finite normal mixture modeling, to provide the group-specific number of components m_g . We then set $M = \sum_g m_g$, combining all outputs from `Mclust`.

For initializing Γ , we rely on both m_g and M , as specified above. We first specify G disjoint sets, denoted as $\{\mathcal{I}_1, \dots, \mathcal{I}_G\}$. We have $\mathcal{I}_g \cap \mathcal{I}_{g'} = \emptyset$ for all $g \neq g'$ and $\cup_{g=1}^G \mathcal{I}_g \subset \{1, 2, \dots, M\}$. These are a small set of indices such that $\gamma_{m,g}$ is fixed at 1 for all $m \in \mathcal{I}_g$ at the initial stage of the MCMC. The set \mathcal{I}_g is constructed as $\mathcal{I}_g = \{m + \sum_{t=1}^{g-1} m_t : m \in \{1, 2, \dots, m_g\}\}$. For the first 1000 iterations, we only sample $\gamma_{m,g}$ for $m \notin \mathcal{I}_g$, and then for all m afterwards.

The initialization of the mixture model centers $\boldsymbol{\mu}$ relies on the traditional k-means clustering. We implement the algorithm using the `kmeans` function in R. We set m_g as the target number of partitions for each group, which returns centroids of the partitions $\boldsymbol{\mu}_g$. We collect all centroids, which serve as our initialization for $\boldsymbol{\mu}_g$'s and thus, $\boldsymbol{\mu}$. The initialization of the standard deviation $\boldsymbol{\sigma}$ also uses the traditional k-means clustering. Similar to the initialization of $\boldsymbol{\mu}$, the `kmeans` function returns the within-cluster sum of squares (WSS) with one

component per cluster. We then calculate $\sigma_g = \sqrt{WSS/(m_g - 1)}$ and collect all σ_g to serve as our initialization of σ . For any possible values where $\sigma_m = 0$, we set it to be 1.

4.5 Selection of K in Neural Net Link Case

It is important to select K that will optimize our model's performance. In our analysis, we employ a cross-validation-based approach, using the predictive log-likelihood on a held-out test set. Ideally, we select K such that it optimally balances complexity and predictive performance. To determine the best K , we first specify a sequence of choices and evaluate their performance based on the predictive log-likelihood.

For each model fitting, our MCMC algorithm will generate B posterior samples. Given a set of these samples, we compute the log-likelihood $ll_K^{(b)}$ under each K for each posterior b from $b = 1, \dots, B$, based on the following equation:

$$\begin{aligned} ll_K^{(b)} = & \sum_{i=1}^N \sum_{g=1}^G \delta_i \log \left(c_g^{(b)}(\mathbf{x}_i) + \{1 - c_g^{(b)}(\mathbf{x}_i)\} \sum_m \pi_{i,m,g}^{(b)} (1 - a_{i,m}^{(b)}) \right) \\ & + (1 - \delta_i) \log \left(\{1 - c_g^{(b)}(\mathbf{x}_i)\} \sum_m \pi_{i,m,g}^{(b)} b_{i,m}^{(b)} \right), \end{aligned}$$

where the superscript (b) denotes b -th posterior sample. For notation, we denote $a_{i,m} = \Phi_m \left(\frac{\log(t_i) - \mu_m}{\sigma_m} \right)$ and $b_{i,m} = \frac{1}{t_i \sqrt{2\pi\sigma_m^2}} \exp \left\{ -\frac{(\log(t_i) - \mu_m)^2}{2\sigma_m^2} \right\}$. Then the predictive log-likelihood is averaged over all B samples as $ll_K^{\text{pred}} = \frac{1}{B} \sum_{b=1}^B ll_K^{(b)}$. Each replication may select a different K that maximizes the predictive log-likelihood. This approach allows for a holistic data-driven selection of K .

4.6 Inference on survival probability for treatment effect

In a survival analysis, the conditional average treatment effect (CATE) at horizon h , a pre-specified cutoff time point, between treatments g and g' is defined as: $\text{CATE}_{gg'}^{(h)}(\mathbf{x}) = \mathbb{E}[m_g(T) - m_{g'}(T) \mid \mathbf{X} = \mathbf{x}]$, where $m_g(T)$ is the survival measure (Cui et al., 2023). In this paper, we use the restricted mean survival time (RMST) as the measure of survival. RMST quantifies the average survival time due to treatment, offers straightforward estimation of differences, and enhances the clinical interpretability of treatment effects for patients and decision-makers (Royston and Parmar, 2013; Tian et al., 2014). Under this survival outcome, the survival measure becomes $m_g(T) = T \wedge h$, which is the minimum time between the random variable T and the horizon h . Based on Royston and Parmar (2013), the group-specific RMST is the area under the survival curve $S_g(t)$ from $t = 0$ to $t = h$: $\text{RMST}_g(h) = \mathbb{E}_g[T \wedge h] = \int_0^h S_g(t)dt$. Thus, the CATE based on RMST is

$$\zeta_{gg'}^{(h)}(\mathbf{x}) = \mathbb{E}_g(T \wedge h \mid \mathbf{x}) - \mathbb{E}_{g'}(T \wedge h \mid \mathbf{x}).$$

In the mixture cure model, the expected RMST for susceptible patients is

$$\begin{aligned} \mathbb{E}_g[T \wedge h \mid \mathbf{x}_i] &= \int_0^h S_g(t)dt = \int_0^h [c_g(\mathbf{x}_i) + \{1 - c_g(\mathbf{x}_i)\}S_{g,u}(t)]dt \\ &= c_g(\mathbf{x}_i)h + \{1 - c_g(\mathbf{x}_i)\} \sum_m \pi_m \int_0^h t \left[\frac{1}{t\sigma_m} \phi_m \left(\frac{\log(t) - \mu_m}{\sigma_m} \right) \right] dt \end{aligned}$$

To approximate the integral, we apply the Monte Carlo method. In that, we generate N_{mc} Monte Carlo samples $T_{m,1}, \dots, T_{m,N_{mc}}$ from the log-normal distribution with parameters μ_m and σ_m for each m . The Monte Carlo approximation for the integral would be

$\int_0^h t \frac{1}{t\sigma_m} \phi_m \left(\frac{\log(t) - \mu_m}{\sigma_m} \right) dt \approx \frac{1}{N_{mc}} \sum_{s=1}^{N_{mc}} (T_{m,s} \wedge h)$. Thus the RMST can be calculated as

$$\text{RMST}_g(h) \approx c_g(\mathbf{x}_i)h + \{1 - c_g(\mathbf{x}_i)\} \sum_m \pi_m \left[\frac{1}{N_{mc}} \sum_{s=1}^{N_{mc}} (T_{m,s} \wedge h) \right].$$

Although our primary analysis focuses on RMST, we also consider the CATE for survival probability. We describe the measurement of survival, conditional expectation, and Monte Carlo approximation for the survival probability in the supplementary Section S4.

Marginal best linear projection: Building on Cui et al. (2023), Chang and Roy (2025) extended the best linear projections (BLP) approach by incorporating a thresholding step within a Bayesian framework. In this paper, a data-partitioning strategy is further added for assessing robustness in addition to applying thresholded MBLPs marginally for each predictor.

We modify the linear projection approach from Semenova and Chernozhukov (2021); Cui et al. (2023) for the inference on $\zeta(\cdot)$ within our Bayesian setting in our numerical experiment by employing a combination of data partitioning and marginal univariate regressions. The marginal BLP (MBLP) for predictor p is

$$\{\beta_{0,p}^*, \beta_p^*\} = \operatorname{argmin}_{\beta_{0,p}, \beta_p} \mathbb{E} [(\zeta(\mathbf{x}_i) - \beta_{0,p} - x_{i,p}\beta_p)^2].$$

For the b -th posterior sample, we obtain $\zeta_{gg',b}(\mathbf{x}_i)$ based on the posterior samples of the survival probability or RMST for the i -th patient. We next perform separate univariate regressions for $\zeta_{gg',b}(\mathbf{x}_i)$ on $x_{i,p}$, providing the estimated MBLP coefficients for the p -th predictor β_p^* . This procedure is repeated for each subgroup, obtained by weighted k-means clustering applying the `ewkm` function from the `wskm` package (Williams et al., 2020).

Furthermore, we consider the thresholded MBLP coefficients (Chang and Roy, 2025) and

compute their credible intervals to assess the importance of predictors. For a given predictor p and threshold t , we compute $s_{p,t} = \frac{1}{B} \sum_{b=1}^B \mathbf{1}\{|\beta_p^{(b)}| > t\}$, the proportion of coefficients falling outside of the interval $(-t, t)$ across all the posterior samples. We examine the decay of $s_{p,t}$ as t increase, with a slower decay indicating greater importance. We demonstrate the effectiveness of this approach in Section 5.2.

5 Simulation

In this section, we assess our proposed method by estimating model parameters using the training data and calculating predicted mean squared errors of the RMST on a pre-determined horizon h . We only present the results of RMST in the subsequent subsections, while including the results of survival probability in the supplementary material. The mean square error (MSE) for treatment-groups pair (g, g') is defined as

$$\frac{1}{|T_r|} \sum_{i \in T_r} \left[\left(\hat{\zeta}_{gg'}(h \mid \mathbf{x}_i) - \zeta_{gg'}(h \mid \mathbf{x}_i) \right) \right]^2,$$

where T_r represent the test set for the r -th replication. We then compute the median MSE over r for each method. Here, $\hat{\zeta}_{gg'}(h \mid \mathbf{x}_i)$ represents the posterior mean for the Bayesian implementations of CATE estimate of the RMST. Likewise $\zeta_{gg'}(h \mid \mathbf{x}_i)$ is the point estimate for the frequentist implementations of the CATE estimate. We conduct two simulations with 50 replicated datasets.

Our model incorporates two key structural features: (1) the presence of a cure fraction, and (2) multiple treatment arms. Furthermore, our model facilitates a direct estimation of RMST, thereby simplifying the treatment effect estimation with multiple treatments. Taking these into account, among existing approaches, only **flexsurvcure** (Amdahl, 2022) is found

to be suitable for comparison as it also allows to get the RMST with multiple treatment arms. For example, `grf` supports RMST-based treatment effect estimation only in two-treatment settings; it produces an error otherwise and is also not designed to handle the cure aspect. Thus, we only compare our estimates with the mixture cure model from `flexsurvcure`, employing a log-normal accelerated failure time (AFT) model for the survival component. To incorporate multi-treatment design, we fit this cure model package following the S-learning approach, where we model the outcome $S(t_i | \mathbf{x}_i) = f(\mathbf{x}_i, z_{2i}, z_{3i}) + \epsilon_i$, where $z_{2i} = 1$ if i -th subject is treated under the second treatment and zero otherwise; z_{3i} is defined similarly for the third treatment. Consequently, z_{2i} and z_{3i} are both zero if i -th subject is in the first treatment group. For CATE estimation (Amdahl, 2022; Jackson, 2016), `flex_surv_cure` and `predict.flexsurvreg` functions are applied on the training and testing sets, respectively.

We conduct two simulations settings with 50 replicated datasets. In the first simulation, we consider a well-specified case where true survival times were generated from a log-normal distribution, aligning with the assumptions of the fitted model. In the second simulation, we introduce a misspecified setting, where survival times were simulated based on a mixture cure model package.

5.1 Well-specified case

Under this setting, we use a sample size 180 with ($P = 3$) covariates with three equal treatment groups. To assess the performance of our model, each dataset is partitioned into training and testing sets with a 67/33 split. We consider three scenarios for our model under different cure rates: high and low. To do this, we introduce an offset in the susceptible probability. For both high and low cure rate setting, we set the offset as 0 and 0.4 for all

patients, respectively. As the the offset increases, it can be seen that the probability of being cured decreases.

For data generation, we set $M = 9$. This number is selected from applying our component selection process from Section 4.4 to the AALL0434 disease-free survival in years. The covariates were independently sampled from a uniform distribution. For the weights, each element β^0 is drawn independently from a normal distribution $\text{Normal}(0, 0.1^2)$. The basis inclusion indicators Γ^0 were binary variables generated from a Bernoulli distribution $\text{Bernoulli}(0.6)$. To generate μ^0 and σ^0 , we use a similar approach as discussed in Section 4.4, where we use k -means clustering based on M . We then generate the coefficients of the susceptible probability Λ^0 independently from $\text{Unif}(-2, 0)$. We also consider two other distributional settings, $\text{Unif}(-1, 0)$ and $\text{Unif}(-2, 1)$, and include the results in the supplementary Tables S1 and S2 for survival probability and RMST estimations, respectively.

To generate survival times, we first compute the cure probabilities for all subjects following the model in (2) with three predictors. Each patient is then classified as either cured or susceptible based on these probabilities. The survival times of the cured individuals will technically be censored, and censoring times are generated separately as discussed below. For susceptible patients, survival times are generated from randomly selecting a mixture component and sampling from a log-normal distribution with parameters μ_m^0, σ_m^0 . We then draw censoring times from the exponential distribution with rate 0.05, and set the maximum follow-up time to $t = 25$. Each individual's observed survival time is determined as the minimum of the generated survival time and the censoring time. We show the described steps in Algorithm S1 provided in the supplementary material.

To clearly illustrate performance differences, mean squared errors (MSEs) are multiplied

Table 2: Comparing mean squared errors for RMST between the proposed methods and Flexible Parametric Cure Models method, based on 50 replications under $\lambda_{g,p} \sim \text{Unif}(-2, 0)$. The reported errors are the medians over all replications.

	High Cure Rate			Low Cure Rate		
	ζ_{21} MSE	ζ_{31} MSE	ζ_{32} MSE	ζ_{21} MSE	ζ_{31} MSE	ζ_{32} MSE
MC Linear	2.46	0.77	2.41	16.64	1.28	15.51
MC Nonlinear $K = 4$	2.34	0.73	2.37	16.48	1.31	15.61
MC Nonlinear $K = 6$	2.46	0.75	2.42	17.01	1.51	15.91
MC Nonlinear $K = 8$	2.45	0.82	2.50	17.08	1.44	16.02
MC Nonlinear $K = 13$	2.38	0.79	2.48	16.93	1.37	16.04
MC Nonlinear $K = 18$	2.44	0.71	2.57	16.84	1.83	15.69
MC Nonlinear $K = K_{CV}$	2.28	0.78	2.53	16.47	1.48	15.93
flexsurvcure	5.86	2.35	7.35	36.09	5.58	35.85

by 100. The results presented in Table 2 indicate that the proposed method using either the linear or non-linear latent links consistently outperform the flexible parametric cure model in estimating the treatment effect of RMST across ζ_{21} , ζ_{31} , and ζ_{32} in both the high and low cure rate setting. Specifically, the median mean squared errors (MSEs) for all proposed methods were substantially lower with differences particularly pronounced under the low cure rate scenario. When using cross-validation for the nonlinear latent link, our method demonstrated robust performance across different scenarios. Notably, it achieved the lowest median MSE for ζ_{21} for both scenarios. These findings highlight the advantage of selection through cross-validation, suggesting that the $K = K_{CV}$ method effectively balances model complexity and estimation accuracy across the two cure rate conditions.

5.2 Misspecified case

In the well-specified case, the true survival times are generated following our proposed model. For the misspecified case, the survival times are generated closely mimicking the AALL0434 clinical trial data. This allows us to evaluate our model under unknown, real-world complexi-

ties. We also carefully set the simulation parameters so that the group-specific Kaplan-Meier curves of the simulated survival data for the high-cure scenario closely resemble those observed in our motivating clinical trial, as illustrated in Figure 1. We show an example of the curves from the mis-specified simulation in Figure S1 in the supplementary material.

For this simulation, we use the observed values for age, white blood cell count, sex, and CNS status. Survival times are generated based on the first three covariates, with CNS status excluded from the model.

First, we partition the data into M subsets of the AALL0434 dataset and fit M cure models, assuming a log-normal distribution with the `cuRe` R package (Lasse Hjort Jakobsen, 2023). Each model is specified as $c_m(\mathbf{x}_i) + \{1 - c_m(\mathbf{x}_i)\}S_{m,u}(t_i)$, where the cure probability is calculated from $c_m(\mathbf{x}_i) = \text{logit}(\lambda_{m,0} + \sum_{p=1}^P \mathbf{x}_i^T \lambda_{m,p})$ and $S_{m,u}(t_i) = 1 - \Phi((\log(t_i) - \mu_{i,m}) / \sigma_m)$ for each m -th partition. We specifically set $\mu_{i,m}$ to be a linear combination of the predictors and some coefficients such that $\mu_{i,m} = \xi_{0,m} + \boldsymbol{\xi}_m^T \mathbf{x}_i$. Each model returns three outputs: 1) coefficients $\{\lambda_{0,m}, \boldsymbol{\lambda}_m\}$ for the cure probability, 2) coefficients $\{\xi_{0,m}, \boldsymbol{\xi}_m\}$ for $\mu_{i,m}$, and 3) one constant value as σ_m . We borrow the second and third outputs, but we continue to generate the cure probability based on the uniform distribution over $(-2, 0)$ for $\boldsymbol{\Lambda}^0$ in order to introduce heterogeneity across groups. Results for two other choices $\text{Unif}(-1, 0)$ and $\text{Unif}(-2, 1)$ are included in supplementary Tables S3 and S4 for survival probability and RMST estimations, respectively.

We still specify $\boldsymbol{\beta}_0$ and $\boldsymbol{\Gamma}_0$ in the same manner as the first simulation setting. Additionally, the offsets for the different cure rate settings are kept the same. For survival time generation, we again classify each patient as either cured or susceptible, using their cure probabilities. For susceptible patients, we generate the survival time from the log-normal distribution

using $\mu_{i,m}$ and σ_m from the `cuRe` package. For censoring times, we still use the exponential distribution with rate 0.05, but with a maximum follow-up time of $h = 5$. We then use the minimum between the generated survival times and the censoring times as each patient's final observed survival time. The algorithm used to generate these times is shown in Algorithm S2 of the supplementary material.

Table 3: Comparing mean squared errors for RMST between the proposed methods and the Flexible Parametric Cure Models method, based on 50 replications under misspecified data generation with $\lambda_{g,p} \sim \text{Unif}(-2, 0)$. The reported errors are the medians over all replications.

	High Cure Rate			Low Cure Rate		
	ζ_{21} MSE	ζ_{31} MSE	ζ_{32} MSE	ζ_{21} MSE	ζ_{31} MSE	ζ_{32} MSE
MC Linear	4.09	6.46	8.44	7.34	7.29	10.12
MC Nonlinear $K = 4$	3.32	4.01	4.56	6.60	6.75	10.41
MC Nonlinear $K = 6$	3.34	2.89	5.25	6.90	6.72	10.66
MC Nonlinear $K = 8$	3.82	4.04	7.82	7.44	6.19	10.82
MC Nonlinear $K = 13$	4.32	5.02	8.22	8.29	8.23	11.39
MC Nonlinear $K = 18$	3.10	5.89	12.31	8.65	7.81	13.51
MC Nonlinear $K = K_{CV}$	3.57	3.49	8.78	6.92	6.82	10.45
flexsurvcure	12.04	14.88	12.97	14.05	21.83	21.45

Similar to the results of our first simulation setting, Table 3 also shows that our proposed method performs better than the cure model in `flexsurvcure`. Median mean squared errors (MSEs) are consistently lower, underscoring our model's ability to capture nonlinearities effectively. We see that, compared to the linear link, using the nonlinear link shows improved accuracy for most cases. Under the high cure rate scenario, our method using $K = 4$ and $K = 6$ bases usually exhibits the lowest MSEs across all the cases. Under the low cure rate scenario, the differences among our method becomes minimal. The $K = K_{CV}$ approach remains competitive, ensuring robustness and adaptive advantage of cross-validation in the selection of K .

Since the survival outcome depends on only the first three predictors, we turn to our

Table 4: Comparison of thresholding-based $s_{p,t}$ -values for $\widehat{\zeta}_{31}$, $\widehat{\zeta}_{21}$, and $\widehat{\zeta}_{32}$ for different choices of thresholds (t), and predictors in the high cure rate setting for $N = 961$. The thresholding levels are given in the first column. The generated outcomes are independent of the CNS Status predictor, shown in italics. The exclusion proportions are based on 50 replicated datasets.

	Age	WBC	Sex	<i>CNS Status</i>	Age	WBC	Sex	<i>CNS Status</i>	Age	WBC	Sex	<i>CNS Status</i>
Threshold	$\widehat{\zeta}_{21}$				$\widehat{\zeta}_{31}$				$\widehat{\zeta}_{32}$			
0.00	1.00	1.00	1.00	1.00	1.00	1.00	1.00	1.00	1.00	1.00	1.00	1.00
0.05	0.43	0.45	0.23	0.24	0.40	0.39	0.22	0.23	0.45	0.44	0.24	0.22
0.10	0.25	0.26	0.13	0.12	0.22	0.21	0.14	0.11	0.24	0.23	0.13	0.10
0.15	0.17	0.17	0.10	0.08	0.15	0.14	0.11	0.07	0.15	0.14	0.09	0.07
0.20	0.12	0.12	0.08	0.06	0.10	0.10	0.09	0.05	0.10	0.10	0.07	0.05
0.25	0.09	0.08	0.07	0.04	0.08	0.07	0.08	0.03	0.07	0.07	0.06	0.03
0.30	0.07	0.06	0.05	0.03	0.06	0.05	0.07	0.02	0.05	0.05	0.05	0.03
0.35	0.06	0.05	0.04	0.02	0.05	0.04	0.06	0.02	0.04	0.04	0.04	0.02
0.40	0.05	0.04	0.04	0.02	0.04	0.03	0.05	0.01	0.03	0.03	0.03	0.01

Table 5: Comparison of MBLP with data partitions for $\widehat{\zeta}_{31}$, $\widehat{\zeta}_{21}$, and $\widehat{\zeta}_{32}$ in the high cure rate setting for $N = 961$. The generated outcomes are independent of the CNS Status predictor, shown in italics. The exclusion proportions are based on 50 replicated datasets.

The thresholding levels	ζ_{21}				ζ_{31}				ζ_{32}			
	Age	WBC	Sex	<i>CNS Status</i>	Age	WBC	Sex	<i>CNS Status</i>	Age	WBC	Sex	<i>CNS Status</i>
	Partition 1				Partition 2				Partition 3			
0.05	0.66	0.70	0.47	0.40	0.62	0.64	0.42	0.38	0.70	0.72	0.42	0.39
0.15	0.35	0.42	0.22	0.15	0.30	0.35	0.19	0.14	0.36	0.42	0.18	0.10
0.25	0.20	0.29	0.14	0.08	0.17	0.23	0.13	0.08	0.19	0.28	0.10	0.05
0.35	0.13	0.21	0.10	0.05	0.10	0.17	0.10	0.04	0.11	0.21	0.06	0.03
0.40	0.11	0.19	0.09	0.04	0.08	0.14	0.09	0.03	0.09	0.18	0.05	0.02
	Partition 4				Partition 1				Partition 2			
0.05	0.69	0.68	0.60	0.45	0.64	0.63	0.48	0.38	0.71	0.69	0.63	0.46
0.15	0.40	0.40	0.26	0.14	0.35	0.33	0.18	0.12	0.41	0.38	0.26	0.12
0.25	0.26	0.26	0.13	0.05	0.22	0.20	0.10	0.05	0.28	0.24	0.14	0.05
0.35	0.19	0.18	0.07	0.03	0.14	0.14	0.07	0.03	0.20	0.16	0.09	0.03
0.40	0.16	0.15	0.06	0.02	0.12	0.12	0.05	0.02	0.17	0.14	0.07	0.02
	Partition 3				Partition 4				Partition 1			
0.05	0.69	0.67	0.54	0.40	0.66	0.60	0.48	0.34	0.74	0.68	0.57	0.42
0.15	0.40	0.39	0.24	0.16	0.35	0.33	0.24	0.12	0.44	0.38	0.26	0.14
0.25	0.26	0.27	0.14	0.09	0.21	0.22	0.15	0.07	0.28	0.25	0.14	0.07
0.35	0.18	0.20	0.09	0.05	0.14	0.16	0.10	0.04	0.18	0.18	0.09	0.04
0.40	0.16	0.18	0.07	0.04	0.12	0.14	0.09	0.03	0.15	0.16	0.07	0.03
	Partition 2				Partition 3				Partition 4			
0.05	0.73	0.68	0.43	0.44	0.65	0.65	0.38	0.39	0.75	0.71	0.46	0.43
0.15	0.42	0.39	0.20	0.17	0.37	0.35	0.16	0.15	0.44	0.41	0.20	0.16
0.25	0.28	0.26	0.12	0.10	0.25	0.23	0.11	0.09	0.29	0.28	0.11	0.09
0.35	0.21	0.19	0.08	0.06	0.19	0.17	0.09	0.06	0.21	0.22	0.07	0.06
0.40	0.19	0.16	0.07	0.05	0.17	0.15	0.08	0.05	0.18	0.19	0.06	0.05

thresholding-based marginal best linear projection approach from Section 4.6 and analyze the $s_{p,t}$ -values for different predictors (p) and threshold (t), ranging from 0.05 to 0.40. We perform our analysis on a sample size of $N = 961$. Tables S5 and 5 show the $s_{p,t}$ -values based on 50 replications for ζ_{21} , ζ_{31} and ζ_{32} in the high cure rate setting for the full data and the partitions, respectively. We additionally include the thresholding-based results for the low-cure-rate setting in the supplementary as Tables S5 and S6. As expected, the decrease in $s_{p,t}$ with t is the sharpest for CNS status in all partitions, which aligns with their exclusion from the data generation process. The $s_{p,t}$ -values thus provide useful insights into the relationship between the outcome and the predictors.

6 AALL0434 Data Analysis

Following Winter et al. (2018), we include age, sex, white blood cell count, CNS status, and risk status as covariates in the analysis. We apply our proposed method to the AALL0434 dataset, considering both linear and neural network link functions with varying K basis functions up to 30. We determine the optimal model based on predictive log-likelihood, as described in Section 4.5. We observe that the predictive likelihood is the best $K = 20$. Thus, our following inference results are based on the neural network link with $K = 20$.

The treatment arms, C-MTX, C-MTX combined with nelarabine, HDMTX, and HDMTX combined with nelarabine, are frequently referred to as Treatments 1 through 4, respectively. The treatment outcomes are then quantified in terms of the RMST by evaluating the conditional average treatment effects (CATEs). We also compare estimated survival curves under different covariate levels and treatment regimes. Finally, following Section 4.6, we compute $s_{p,t}$ -values for each covariate corresponding to three treatment contrasts $\hat{\zeta}_{21}$, $\hat{\zeta}_{43}$, and $\hat{\zeta}_{31}$,

both under the full data and two partitions. Here, $\widehat{\zeta}_{31}$ helps to compare the two methotrexate regimens without nelarabine, while $\widehat{\zeta}_{21}$, $\widehat{\zeta}_{43}$ compare the addition of nelarabine to the methotrexate regimens. We also compute the $s_{p,t}$ -values for other three treatment contrasts $\widehat{\zeta}_{31}$, $\widehat{\zeta}_{41}$, and $\widehat{\zeta}_{43}$, and have added them to the supplementary Table S7 and partition-based results in Table S8. Our analysis highlights several key findings into covariate-specific treatment effects and their roles in pediatric leukemia outcomes.

CATE (RMST in years) comparison: We also evaluate covariate-specific treatment effects by plotting the estimated CATEs with 95% credible bands against the continuous predictors WBC and age, separately, while fixing other covariates at their sample medians, similar to Cui et al. (2023). Figure 3 illustrates the CATEs as a function of WBC count. In the comparison for HDMTX versus C-MTX in Figure 3a, HDMTX shows a small benefit for low WBC counts, but this is reversed with increasing WBC, favoring C-MTX at higher counts. In Figure 3b, the addition of nelarabine to C-MTX shows a slight benefit across all WBC counts. In contrast, adding nelarabine to HDMTX demonstrates a steadily increasing RMST benefit as WBC count rise, as shown in Figure 3c. This suggests patients may benefit from HDMTX combined with nelarabine than just HDMTX. Overall, higher WBC counts show that C-MTX may be preferable over HDMTX, and the addition of nelarabine is also beneficial, particularly when paired with HDMTX.

Likewise, we plot the CATEs as a function of age in Figure 4. In the comparison between HDMTX and C-MTX, shown in Figure 4a, younger patients experience little RMST benefit with HDMTX, with the CATE gradually decreasing with age. This suggests that HDMTX may be more effective than C-MTX in younger children, but the advantage diminishes in older patients with a preference towards C-MTX. Figures 4a and 4c compare the addition

of nelarabine to the methotrexate regimes. For the comparison of C-MTX with and without nelarabine, younger patients show a higher benefit of C-MTX with nelarabine, but this effect declines with age, reaching zero at higher ages. In contrast, the comparison of HDMTX with versus without nelarabine shows a nearly flat line across, with values close to zero. This indicates that adding nelarabine to these regimes yields little to no additional RMST benefit regardless of patient age. Overall, these results suggest that age modestly affects treatment strategies, particularly comparing C-MTX to HDMTX. However, the benefit of nelarabine is minimal in older patients.

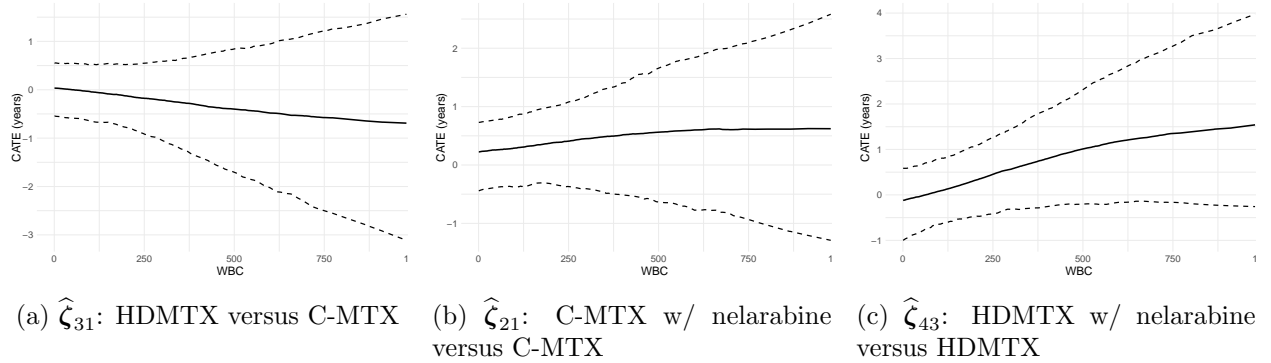


Figure 3: Estimated CATEs (RMST in years) versus WBC count ($x1000\mu\text{L}$) and 95% confidence bands (dash lines), with all other covariates set to their median value. CATEs are estimated using our proposed group-specific mixture cure model with neural network links, setting $K = 20$ and 1,000 posterior samples to derive estimates and confidence bands for different treatment pairs. The data are from the AALL0434 clinical trial with 1022 patients, comparing different treatment arms. Covariates include age (years) as the continuous predictor; sex (0 = female, 1 = male), CNS status (0 = CNS status 1, 1 = CNS status 2), and risk group (0 = low risk, 1 = moderate risk, 2 = high risk) as categorical variables.

Estimated survival curves comparison: In this next comparison, we obtain the estimated DFS survival curves for all subjects in the dataset by applying our proposed CV-selected non-linear mixed-cure model under different treatment group settings. Then we stratify the subjects based on a specific covariate and plot the group-specific average estimated survival curves to compare. The results are shown in Figures S4 through S6.

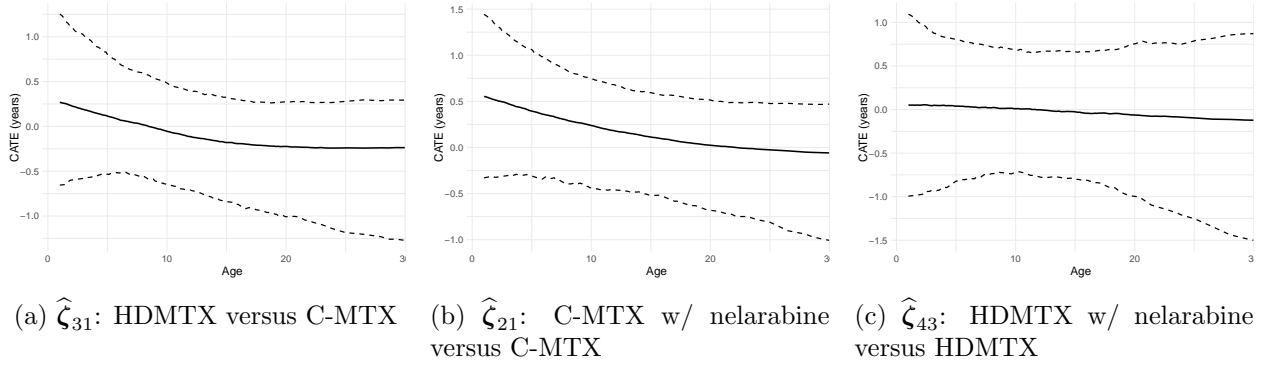


Figure 4: Estimated conditional average treatment effects (RMST in years) versus age (in years) and 95% confidence bands (dashed lines), with all other covariates set to their median value. CATEs are estimated using our proposed group-specific mixture cure model with neural network links, setting $K = 20$ and 1,000 posterior samples to derive estimates and confidence bands for different treatment pairs. The data are from the AALL0434 clinical trial with 1022 patients, comparing different treatment arms. Covariates include white blood cell count ($\times 1000 \mu L$) as the continuous predictor; sex (0 = female, 1 = male), CNS status (0 = CNS status 1, 1 = CNS status 2), and risk group (0 = low risk, 1 = moderate risk, 2 = high risk) as categorical variables.

In Figure S4 stratifies survival by WBC count using μL as the boundary between low and high count. Among patients with high WBC, the survival curves show more separation across treatment groups. In contrast, for low WBC patients, the survival curves across all treatment groups were closely aligned, with C-MTX with nelarabine having slightly higher survival probabilities. This shows the difference in area between two survival curves is smaller in low WBC count patients, suggesting that the treatment effect for RMST is larger for high WBC count patients. This aligns with the results found in our CATE comparison plots for WBC count.

Next, we look at patients stratified by age with 10 years as the cutoff in Figure S2. Among younger patients, we see that the treatment arms with nelarabine have the highest survival probabilities than their non-nelarabine counterparts. In contrast, older patients show higher survival probabilities with C-MTX treatments. When we compare the difference in areas between survival curves, we see that the difference is relatively the same between the both

age groups. This indicates that the RMST treatment effect between age is actually the same and doesn't change as age increases, once again supported by our CATE comparsion for age.

Lastly, Figure S6 stratifies survival by risk group. When looking at specifically the survival curves between the low and moderate risk group, we see the difference in area between HDMTX and C-MTX is much larger in the low risk group. This means that low-risk patients survival analysis comparing low versus moderate risk revealed significantly larger area differences in low-risk patients, showing a larger preference towards HDMTX. In contrast, the arms with nelarabine are more beneficial to moderate risk patients.

Taken together, these stratified survival curves further confirm that treatment effects are not uniform across patient subgroups. When comparing the difference in areas between survival curves, our findings generally align with the results given by our CATE estimation plots.

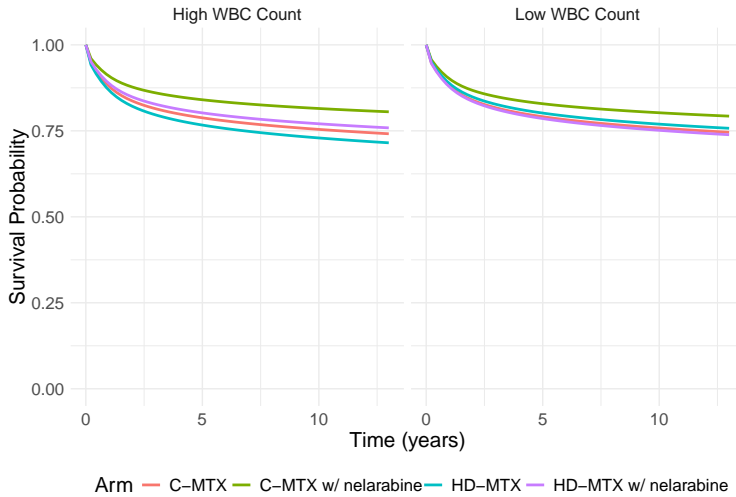


Figure 5: Estimated treatment group-specific survival curves stratified by high and low WBC count applying our proposed mixture-cure model under different methotrexate regimens and with/without nelarabine. Survival curves are estimated using our proposed mixture cure model using neural network links, setting $K = 20$ and 1,000 posterior samples to obtain survival probabilities at equally separated time points from $t = 0$ to $t = 13$. We stratify WBC count by defining high WBC count as having a count of at least $50,000 \mu\text{L}$ (the sample median). We examine the difference in areas between two treatment curves.

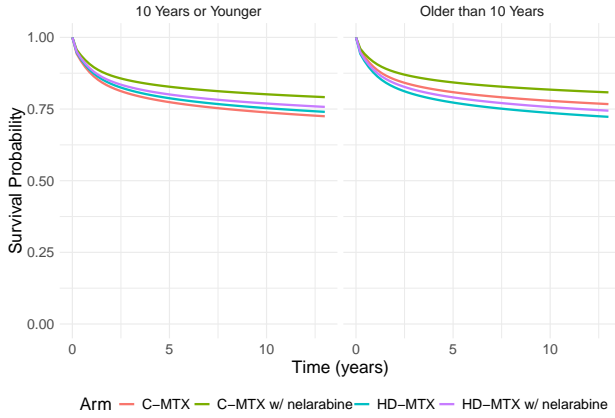


Figure 6: Estimated covariate-dependent treatment group-specific survival curves stratified by two age groups applying our proposed mixture-cure model under different methotrexate regimens and with/without nelarabine. Survival curves are estimated using our proposed mixture cure model using neural network links, setting $K = 20$ and 1,000 posterior samples to obtain survival probabilities at equally separated time points from $t = 0$ to $t = 13$. We stratify age by defining older patients as older than 10 years.

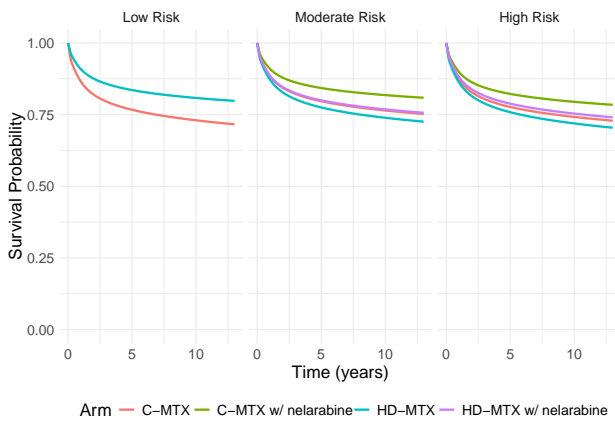


Figure 7: Estimated covariate-dependent treatment group-specific survival curves stratified by risk groups applying our proposed mixture-cure model under different methotrexate regimens and with/without nelarabine. Survival curves are estimated using our proposed mixture cure model using neural network links, setting $K = 20$ and 1,000 posterior samples to obtain survival probabilities at equally separated time points from $t = 0$ to $t = 13$.

MBLP comparison: The $s_{p,t}$ values, representing the marginal importance of each predictor (p) across different thresholds (t), are presented in Table 6 for the full dataset and two identified partitions. Three predictors emerge as particularly influential: WBC count, age,

Table 6: The $s_{p,t}$ -values for $\hat{\zeta}_{31}$, $\hat{\zeta}_{21}$, and $\hat{\zeta}_{43}$ under different choices of thresholds (t) and predictors for the AALL0434 dataset. We present the thresholding results for the full data and the different data partitions.

	Full-data						Partition 1						Partition 2					
	Age	CNS Status	Sex	WBC Count	Low Risk	High Risk	Age	CNS Status	Sex	WBC Count	Low Risk	High Risk	Age	CNS Status	Sex	WBC Count	Low Risk	High Risk
Threshold	$\hat{\zeta}_{31}$																	
0.05	0.97	0.99	0.95	1.00	0.99	0.96	0.98	1.00	0.95	1.00	0.99	0.96	0.98	0.98	0.94	1.00	0.98	0.96
0.15	0.92	0.98	0.85	0.98	0.97	0.88	0.95	0.99	0.86	0.99	0.98	0.88	0.94	0.95	0.83	0.99	0.96	0.89
0.25	0.87	0.95	0.77	0.97	0.95	0.80	0.91	0.98	0.80	0.98	0.96	0.82	0.90	0.92	0.72	0.99	0.94	0.82
0.35	0.81	0.93	0.68	0.95	0.93	0.73	0.88	0.95	0.73	0.97	0.94	0.74	0.85	0.87	0.62	0.98	0.91	0.75
0.40	0.80	0.92	0.62	0.95	0.92	0.69	0.87	0.94	0.68	0.97	0.93	0.71	0.84	0.85	0.58	0.97	0.89	0.70
	$\hat{\zeta}_{21}$																	
0.05	0.98	0.97	0.97	0.97	0.95	0.96	0.97	0.96	0.97	0.97	0.95	0.95	0.98	0.96	0.98	0.97	0.95	0.95
0.15	0.94	0.88	0.92	0.91	0.86	0.86	0.92	0.89	0.91	0.91	0.85	0.86	0.93	0.87	0.94	0.91	0.86	0.87
0.25	0.87	0.79	0.86	0.86	0.77	0.77	0.86	0.82	0.83	0.85	0.76	0.78	0.89	0.78	0.89	0.83	0.79	0.77
0.35	0.83	0.71	0.80	0.80	0.69	0.67	0.79	0.74	0.75	0.80	0.68	0.69	0.83	0.69	0.83	0.78	0.72	0.69
0.40	0.80	0.67	0.76	0.77	0.64	0.62	0.77	0.70	0.72	0.77	0.64	0.65	0.81	0.65	0.80	0.76	0.68	0.66
	$\hat{\zeta}_{43}$																	
0.05	0.97	0.97	0.95	1.00	0.97	0.96	0.98	0.98	0.95	1.00	0.99	0.96	0.97	0.95	0.95	1.00	0.96	0.96
0.15	0.91	0.91	0.84	1.00	0.93	0.88	0.94	0.94	0.86	1.00	0.98	0.88	0.91	0.86	0.86	1.00	0.90	0.88
0.25	0.86	0.83	0.76	1.00	0.88	0.80	0.89	0.88	0.79	1.00	0.97	0.81	0.84	0.78	0.77	1.00	0.83	0.79
0.35	0.80	0.77	0.67	1.00	0.84	0.72	0.83	0.82	0.70	1.00	0.94	0.73	0.78	0.69	0.70	0.99	0.76	0.72
0.40	0.77	0.73	0.63	1.00	0.82	0.68	0.81	0.80	0.67	1.00	0.94	0.69	0.74	0.65	0.65	0.99	0.73	0.68

and low versus moderate risk. WBC exhibits the highest importance across treatment effects $\hat{\zeta}_{31}$ and $\hat{\zeta}_{43}$, while age is the most important for $\hat{\zeta}_{21}$. These results reaffirm prior findings by Liu et al. (2022), emphasizing WBC count as a crucial prognostic marker in pediatric leukemia. Additionally, CNS status and low versus moderate risk classification jointly rank second in importance for $\hat{\zeta}_{31}$. In $\hat{\zeta}_{43}$, low versus moderate risk holds second place, followed by age.

We further inspect predictor influences on treatment response through the MBLP coefficients in Table 7. WBC count consistently demonstrated a negative coefficient for $\hat{\zeta}_{31}$,

Table 7: The MBLP coefficients for predictors in AALL0434 for treatment effects $\hat{\zeta}_{31}$, $\hat{\zeta}_{21}$, and $\hat{\zeta}_{43}$ for RMST with their 95% credible interval. Treatment groups are based on the usage of only C-MTX (group 1), C-MTX with nelarabine (group 2), HDMTX (group 3), and HDMTX with nelarabine (group 4).

Predictor	Full-data			Partition 1			Partition 2		
	$\hat{\zeta}_{31}$	$\hat{\zeta}_{21}$	$\hat{\zeta}_{43}$	$\hat{\zeta}_{31}$	$\hat{\zeta}_{21}$	$\hat{\zeta}_{43}$	$\hat{\zeta}_{31}$	$\hat{\zeta}_{21}$	$\hat{\zeta}_{43}$
Age	-0.86	-1.01	-0.50	-1.44	-0.81	0.24	-1.24	-0.98	0.10
CNS Status 2 vs 1	-1.29	-0.62	0.54	-1.64	-0.67	0.88	-1.00	-0.60	0.20
Sex	0.48	0.79	0.46	0.55	0.71	0.39	0.42	0.85	0.57
WBC Count	-2.50	0.54	4.24	-2.74	0.41	4.36	-2.83	0.61	4.69
Low vs Moderate Risk	1.21	0.08	-1.58	1.42	-0.19	-2.22	1.09	0.24	-1.19
High vs Moderate Risk	-0.47	0.40	0.32	-0.47	0.30	0.30	-0.50	0.47	0.39

supporting preference for C-MTX over HDMTX, aligning with Dunsmore et al. (2020). Conversely, the positive coefficients in comparisons involving nelarabine suggest patients with elevated WBC counts will have a higher expected survival time from its inclusion. These trends match our CATE and survival curve analyses.

Age, considered second-most influential, shows negative coefficients across all three treatment comparisons, indicating older patients generally benefit more from C-MTX and less from nelarabine, as shown in our CATE comparison. A positive coefficient for $\hat{\zeta}_{31}$ highlights greater benefits of HDMTX for low-risk patients compared to moderate-risk ones, again established by our survival curve comparison. Low-risk patients show slight advantages with the addition of nelarabine in C-MTX regimens; however, the negative coefficient for $\hat{\zeta}_{43}$ indicates HDMTX without nelarabine favors low-risk patients.

These findings emphasize the use of WBC count, age, and risk classification to guide treatment selection and predict survival outcomes in pediatric leukemia. These consistent findings across RMST-based CATE analyses, estimated survival curves, and MBLP reinforce the methodological robustness and clinical relevance of our results. We gain new insights

from these results, as illustrated in the next section.

7 Discussion

We propose a Bayesian mixture cure model to estimate heterogeneous treatment effects in the presence of both long-term survivors and shared treatment mechanisms. Our method flexibly incorporates linear and neural-network link functions, enabling covariate-dependent cure probabilities and individualized mixture weights for survival distributions. Treatment effects are assessed through differences in RMST, with both data partitioning and MBLP to evaluate variable importance. Simulation results demonstrate superior performance of our model over the Flexible Parametric Cure Model method in estimation accuracy for both a well-specified and mis-specified case. When applying our model to the AALL0434 trial data, we uncover hidden patterns of potential treatment effect heterogeneity not identified in prior analyses.

In previous analyses of the AALL0434 trial, standard prognostic variables such as WBC count, age at diagnosis, and risk status were not found to have notable interactions with treatment arm when evaluated using disease-free survival. In our RMST-based evaluation, however, the CATE plots, estimated survival curves, and MBLP analysis all suggest that these predictors could play a meaningful role in estimating treatment effects. According to the results, patients with higher WBC count would preferably be treated with C-MTX over HD-MTX or the addition of nelarabine in order to increase expected survival time. Similarly, older patients derive less benefit from nelarabine, thus refining the earlier observations of Winter et al. (2018) and Dunsmore et al. (2020). RMST provides straightforward and clinically interpretable findings for differences in survival between groups, which may uncover

important prognostic factors overlooked by hazard models (Wu et al., 2025). Our results using CATE plots, estimated survival curves, and MBLP analysis underscore the potential for using RMST-based heterogeneity to guide personalized treatment decisions in T-cell ALL. However, the clinical interpretations using the COG AALL0434 trial data with our novel methods should be considered preliminary and exploratory in nature. In addition to the trial being the first real-world data used with the methods, there are also some caveats within the trial implementation, including some non-random treatment assignments, and certain risk cohorts not having availability to all randomization choices for the entirety of the study (Winter et al., 2018; Dunsmore et al., 2020). However, the covariate-based analysis should be generally valid and this study still portrays the potential benefits of our method for uncovering hidden treatment effect patterns versus standard analyses.

Identifiability is a concern if there is a focus on accurately estimating the cure probabilities. In this paper, our focus was on estimating the treatment effects in terms of overall survival probabilities and RMSTs, and thus, we did not focus on identifying the cure probabilities uniquely. There are works establishing the required identifiability conditions (Hanin and Huang, 2014; Patilea and Van Keilegom, 2020). It is possible to incorporate some of these conditions into our proposed non-parametric mixture-cure model as a future work.

Future research may also consider mixture of experts type models with covariate-dependent survival curves along with covariate-dependent weights (Jordan and Jacobs, 1994; Bishop and Svensén, 2003). Our current model only considers the latter. This extension would add greater flexibility with an added computational cost. Collectively, these extensions hold promise for refining individualized survival prediction and informing more targeted treatment allocation in complex survival settings.

Acknowledgement

This work was supported by the National Institutes of Health [NCTN Statistics & Data Center Grant – U10CA180899; NCTN Operations Center Grant U10CA180886]. Its contents are solely the responsibility of the authors and do not necessarily represent the official views of the NIH. The authors would also like to acknowledge the Children’s Oncology Group ALL Committee for permitting use of the AALL0434 data.

Supplementary Materials for ‘Nonparametric Bayesian Multi-Treatment Mixture Cure Survival Model with Application in Pediatric Oncology’

Peter Chang, John Kairalla, Arkaprava Roy
Department of Biostatistics, University of Florida, United States

S1 Likelihood derivation of the mixture cure model

Here we set $r_g = 1 - c_g$ and can derive the likelihood of the mixture model as follows: for any subjects censored ($\delta_i = 1$), then the likelihood function is

$$\begin{aligned}
p(t_i) \mid \boldsymbol{\pi}, \boldsymbol{\lambda}_g, \mathbf{x}_i, \boldsymbol{\mu}, \boldsymbol{\sigma} &= S_g(t_i) \mid \boldsymbol{\pi}, \boldsymbol{\lambda}_g, \mathbf{x}_i, \boldsymbol{\mu}, \boldsymbol{\sigma} \\
&= P(T > \log(t_i)) = (1 - r_g(\mathbf{x}_i)) + r_g(\mathbf{x}_i) S_{g,u}(t_i) \mid \mathbf{x} \\
&= (1 - r_g(\mathbf{x}_i)) + r_g(\mathbf{x}_i) \int_{t_i}^{\infty} f_u(x \mid \mathbf{x}_i, \boldsymbol{\mu}, \boldsymbol{\sigma}) dx \\
&= (1 - r_g(\mathbf{x}_i)) + r_g(\mathbf{x}_i) \int_{t_i}^{\infty} \sum_m \pi_m \phi_m(x, \mu_m, \sigma_m^2) dx \\
&= (1 - r_g(\mathbf{x}_i)) + r_g(\mathbf{x}_i) \sum_m \pi_m \int_{t_i}^{\infty} \phi_m(x, \mu_m, \sigma_m^2) dx \\
&= (1 - r_g(\mathbf{x}_i)) + r_g(\mathbf{x}_i) \sum_m \pi_m [\Phi_m(\infty, \mu_m, \sigma_m^2) - \Phi_m(t_i, \mu_m, \sigma_m^2)] \\
&= (1 - r_g(\mathbf{x}_i)) + r_g(\mathbf{x}_i) \sum_m \pi_m (1 - \Phi_m(t_i, \mu_m, \sigma_m^2)) \\
&= (1 - r_g(\mathbf{x}_i)) + r_g(\mathbf{x}_i) \sum_m \pi_m \left(1 - \Phi_m \left(\frac{\log(t_i) - \mu_m}{\sigma_m} \right) \right)
\end{aligned}$$

for any subjects uncensored ($\delta_i = 0$), then the likelihood function is

$$\begin{aligned}
p(t_i) \mid \boldsymbol{\pi}, \boldsymbol{\lambda}_g, \mathbf{x}_i, \boldsymbol{\mu}, \boldsymbol{\sigma} &= f(t_i) \mid \boldsymbol{\lambda}_g, \mathbf{x}_i, \boldsymbol{\mu}, \boldsymbol{\sigma} \\
&= - \frac{\partial}{\partial t} S_g(t_i) \mid \boldsymbol{\lambda}_g, \mathbf{x}_i, \boldsymbol{\mu}, \boldsymbol{\sigma} \\
&= - \frac{\partial}{\partial t} (1 - r_g(\mathbf{x}_i)) + r_g(\mathbf{x}_i) S_{g,u}(t_i) \mid \mathbf{x} \\
&= - r_g(\mathbf{x}_i) \frac{\partial}{\partial t} S_{g,u}(t_i) \mid \mathbf{x} \\
&= r_g(\mathbf{x}_i) f_u(t_i) \mid \mathbf{x}_i, \boldsymbol{\mu}, \boldsymbol{\sigma} \\
&= r_g(\mathbf{x}_i) \sum_m \pi_m \frac{1}{t_i \sqrt{2\pi\sigma_m^2}} \exp \left\{ -\frac{(\log(t_i) - \mu_m)^2}{2\sigma_m^2} \right\}
\end{aligned}$$

Here, $f_u(t_i) \mid \mathbf{x}_i, \boldsymbol{\mu}, \boldsymbol{\sigma}$ is the mixture of M components with the components belonging to the lognormal distribution.

Then the likelihood function with both contributions for all subjects becomes

$$\begin{aligned}
p(\mathbf{t} \mid \boldsymbol{\mu}, \boldsymbol{\sigma}, \boldsymbol{\pi}, \boldsymbol{\lambda}, \mathbf{x}) &= \prod_{i=1}^N \prod_{g=1}^G S_g(t_i) \mid \boldsymbol{\lambda}_g, \mathbf{x}_i, \boldsymbol{\mu}, \boldsymbol{\sigma}) \mathbf{1}(\delta_i = 1) + f(t_i) \mid \boldsymbol{\lambda}_g, \mathbf{x}_i, \boldsymbol{\mu}, \boldsymbol{\sigma}) \mathbf{1}(\delta_i = 0) \\
&= \prod_{i=1}^N \prod_{g=1}^G S_g(t_i) \mid \boldsymbol{\lambda}_g, \mathbf{x}_i, \boldsymbol{\mu}, \boldsymbol{\sigma})^{\delta_i} f(t_i) \mid \boldsymbol{\lambda}_g, \mathbf{x}_i, \boldsymbol{\mu}, \boldsymbol{\sigma})^{1-\delta_i} \\
&= \prod_{i=1}^N \prod_{g=1}^G \left[(1 - r_g(\mathbf{x}_i)) + r_g(\mathbf{x}_i) \sum_m \pi_m \left(1 - \Phi_m \left(\frac{\log(t_i) - \mu_m}{\sigma_m} \right) \right) \right]^{\delta_i} \\
&\quad \times \left[r_g(\mathbf{x}_i) \sum_m \pi_m \frac{1}{t_i \sqrt{2\pi\sigma_m^2}} \exp \left\{ -\frac{(\log(t_i) - \mu_m)^2}{2\sigma_m^2} \right\} \right]^{1-\delta_i}
\end{aligned}$$

S2 Posterior sampling derivations

S2.1 Linear link

In this model, for the i -th individual in g -th group, the weights can be written as

$$\pi_{i,m,g} = \frac{\gamma_{m,g} \exp(\mathbf{x}_i^T \boldsymbol{\beta}_m)}{\sum_j \gamma_{j,g} \exp(\mathbf{x}_i^T \boldsymbol{\beta}_j)}.$$

Assume that $\boldsymbol{\mu}$ and $\boldsymbol{\sigma}$ are known.

Let's also do some quick notation for some of the expressions. For the i -th subject:

- $a_{i,m} = \Phi_m \left(\frac{\log(t_i) - \mu_m}{\sigma_m} \right)$. Note that $S_g(t_i) \mid \boldsymbol{\lambda}, \mathbf{x}_i, \boldsymbol{\mu}, \boldsymbol{\sigma} = (1 - r_g(\mathbf{x}_i)) + r_g(\mathbf{x}_i) \sum_m \pi_{i,m,g} (1 - a_{i,m})$
- $b_{i,m} = \frac{1}{t_i \sqrt{2\pi\sigma_m^2}} \exp \left\{ -\frac{(\log(t_i) - \mu_m)^2}{2\sigma_m^2} \right\}$. Note that $f_u(t_i) \mid \mathbf{x}_i, \boldsymbol{\mu}, \boldsymbol{\sigma} = \sum_m \pi_{i,m,g} b_{i,m}$

S2.1.1 Gradient of $\boldsymbol{\beta}_m$

We can write the log-likelihood as:

$$\begin{aligned}
l(\boldsymbol{\beta} \mid \mathbf{t}, \boldsymbol{\mu}, \boldsymbol{\sigma}, \boldsymbol{\lambda}_g, \mathbf{x}_i) &= \sum_{i=1}^N \sum_{g=1}^G \delta_i \log \left((1 - r_g(\mathbf{x}_i)) + r_g(\mathbf{x}_i) \sum_m \pi_{i,m,g} (1 - a_{i,m}) \right) \\
&\quad + (1 - \delta_i) \log \left(r_g(\mathbf{x}_i) \sum_m \pi_{i,m,g} b_{i,m} \right)
\end{aligned}$$

We need to find the derivative of the weights with respect to β_m . For $j = m$:

$$\begin{aligned}
\frac{\partial}{\partial \beta_m} \pi_{i,m,g} &= \frac{\partial}{\partial \beta_m} \frac{\gamma_{m,g} \exp(\mathbf{x}_i^T \beta_m)}{\sum_k \gamma_{k,g} \exp(\mathbf{x}_i^T \beta_k)} \\
&= \frac{\sum_k \gamma_{k,g} \exp(\mathbf{x}_i^T \beta_k) \left(\frac{\partial}{\partial \beta_m} \gamma_{m,g} \exp(\mathbf{x}_i^T \beta_m) \right) - \gamma_{m,g} \exp(\mathbf{x}_i^T \beta_m) \left(\frac{\partial}{\partial \beta_m} \sum_k \gamma_{k,g} \exp(\mathbf{x}_i^T \beta_k) \right)}{\left(\sum_k \gamma_{k,g} \exp(\mathbf{x}_i^T \beta_k) \right)^2} \\
&= \frac{\sum_k \gamma_{k,g} \exp(\mathbf{x}_i^T \beta_k) (\gamma_{m,g} \exp(\mathbf{x}_i^T \beta_m))(\mathbf{x}_i) - \gamma_{m,g} \exp(\mathbf{x}_i^T \beta_m) (\gamma_{m,g} \exp(\mathbf{x}_i^T \beta_m))(\mathbf{x}_i)}{\left(\sum_k \gamma_{k,g} \exp(\mathbf{x}_i^T \beta_k) \right)^2} \\
&= \frac{(\sum_k \gamma_{k,g} \exp(\mathbf{x}_i^T \beta_k) - \gamma_{m,g} \exp(\mathbf{x}_i^T \beta_m)) (\gamma_{m,g} \exp(\mathbf{x}_i^T \beta_m))(\mathbf{x}_i)}{\left(\sum_k \gamma_{k,g} \exp(\mathbf{x}_i^T \beta_k) \right)^2} \\
&= (1 - \pi_{i,m,g}) \pi_{i,m,g} \mathbf{x}_i
\end{aligned}$$

For $j \neq m$:

$$\begin{aligned}
\frac{\partial}{\partial \beta_m} \pi_{i,j,g} &= \frac{\partial}{\partial \beta_m} \frac{\gamma_{j,g} \exp(\mathbf{x}_i^T \beta_j)}{\sum_k \gamma_{k,g} \exp(\mathbf{x}_i^T \beta_k)} \\
&= \frac{\sum_k \gamma_{k,g} \exp(\mathbf{x}_i^T \beta_k) \left(\frac{\partial}{\partial \beta_m} \gamma_{j,g} \exp(\mathbf{x}_i^T \beta_j) \right) - \gamma_{j,g} \exp(\mathbf{x}_i^T \beta_j) \left(\frac{\partial}{\partial \beta_m} \sum_k \gamma_{k,g} \exp(\mathbf{x}_i^T \beta_k) \right)}{\left(\sum_k \gamma_{k,g} \exp(\mathbf{x}_i^T \beta_k) \right)^2} \\
&= \frac{-\gamma_{j,g} \exp(\mathbf{x}_i^T \beta_j) (\gamma_{m,g} \exp(\mathbf{x}_i^T \beta_m))(\mathbf{x}_i)}{\left(\sum_k \gamma_{k,g} \exp(\mathbf{x}_i^T \beta_k) \right)^2} \\
&= -\pi_{i,j,g} \pi_{i,m,g} \mathbf{x}_i
\end{aligned}$$

The score function for β_m is

$$\begin{aligned}
\frac{\partial}{\partial \beta_m} l(\beta \mid \mu, \sigma, \Gamma, \mathbf{t}, \mathbf{x}) &= \\
&\sum_{i=1}^N \sum_{g=1}^G \frac{\delta_i r_g(\mathbf{x}_i)}{S_g(t_i) \mid \lambda, \mathbf{x}_i, \mu, \sigma} \left((\pi_{i,m,g} \mathbf{x}_i) \left((1 - a_{i,m})(1 - \pi_{i,m,g}) - \sum_{j \neq m}^M (1 - a_{i,j}) \pi_{i,j,g} \right) \right) \\
&+ \frac{(1 - \delta_i)}{f_u(t_i) \mid \mathbf{x}_i, \mu, \sigma} (\pi_{i,m,g} \mathbf{x}_i) \left(b_{i,m}(1 - \pi_{i,m,g}) - \sum_{j \neq m}^M b_{i,j} \pi_{i,j,g} \right),
\end{aligned}$$

S2.1.2 Gradient of μ_m

$$l(\boldsymbol{\mu} \mid \mathbf{t}, \boldsymbol{\sigma}, \boldsymbol{\beta}, \boldsymbol{\lambda}_g, \mathbf{x}_i) = \sum_{i=1}^N \sum_{g=1}^G \delta_i \log \left((1 - r_g(\mathbf{x}_i)) + r_g(\mathbf{x}_i) \sum_m \pi_{i,m,g} (1 - a_{i,m}) \right) \\ + (1 - \delta_i) \log \left(r_g(\mathbf{x}_i) \sum_m \pi_{i,m,g} b_{i,m} \right)$$

We need to find the derivative of both $\log \left((1 - r_g(\mathbf{x}_i)) + r_g(\mathbf{x}_i) \sum_j \pi_{i,j,g} (1 - a_{i,j}) \right)$ and $\log \left(r_g(\mathbf{x}_i) \sum_{j=1}^M \pi_{i,j,g} b_{i,j} \right)$.

$$\begin{aligned} \frac{\partial}{\partial \mu_m} \log \left((1 - r_g(\mathbf{x}_i)) + r_g(\mathbf{x}_i) \pi_{i,j,g} (1 - a_{i,j}) \right) \\ = \frac{r_g(\mathbf{x}_i)}{S_g(t_i) \mid \boldsymbol{\lambda}_g, \mathbf{x}_i, \boldsymbol{\mu}, \boldsymbol{\sigma}} \frac{\partial}{\partial \mu_m} \sum_j \pi_{i,j,g} (1 - a_{i,j}) \\ = \frac{r_g(\mathbf{x}_i)}{S_g(t_i) \mid \boldsymbol{\lambda}_g, \mathbf{x}_i, \boldsymbol{\mu}, \boldsymbol{\sigma}} \frac{\partial}{\partial \mu_m} \pi_{i,m,g} (1 - a_{i,m}) \\ = - \frac{r_g(\mathbf{x}_i) \pi_{i,m,g}}{S_g(t_i) \mid \boldsymbol{\lambda}_g, \mathbf{x}_i, \boldsymbol{\mu}, \boldsymbol{\sigma}} \frac{\partial}{\partial \mu_m} a_{i,m} \\ = - \frac{r_g(\mathbf{x}_i) \pi_{i,m,g}}{S_g(t_i) \mid \boldsymbol{\lambda}_g, \mathbf{x}_i, \boldsymbol{\mu}, \boldsymbol{\sigma}} \frac{\partial}{\partial \mu_m} \Phi_m \left(\frac{\log(t_i) - \mu_m}{\sigma_m} \right) \\ = \frac{r_g(\mathbf{x}_i) \pi_{i,m,g}}{\sigma_m S_g(t_i) \mid \boldsymbol{\lambda}_g, \mathbf{x}_i, \boldsymbol{\mu}, \boldsymbol{\sigma}} \phi_m \left(\frac{\log(t_i) - \mu_m}{\sigma_m} \right) \end{aligned}$$

Importantly, $\phi_m \left(\frac{\log(t_i) - \mu_m}{\sigma_m} \right)$ is the Normal PDF, since we are taking the derivative of the normal CDF with respect to μ_m .

$$\frac{\partial}{\partial \mu_m} \log \left(r_g(\mathbf{x}_i) \sum_{j=1}^M \pi_{i,j,g} b_{i,j} \right) = \frac{1}{\sum_{j=1}^M \pi_{i,j,g} b_{i,j}} \frac{\partial}{\partial \mu_m} \left(\sum_{j=1}^M \pi_{i,j,g} b_{i,j} \right)$$

$$\begin{aligned}
&= \frac{\pi_{i,m,g}}{\sum_{j=1}^M \pi_{i,j,g} b_{i,j}} \frac{\partial}{\partial \mu_m} b_{i,m} \\
&= \frac{\pi_{i,m,g}}{\sum_{j=1}^M \pi_{i,j,g} b_{i,j}} \frac{\partial}{\partial \mu_m} \left(\frac{1}{t_i \sqrt{2\pi\sigma_m^2}} \exp \left\{ -\frac{(\log(t_i) - \mu_m)^2}{2\sigma_m^2} \right\} \right) \\
&= \frac{\pi_{i,m,g}}{\sum_{j=1}^M \pi_{i,j,g} b_{i,j}} \frac{1}{t_i \sqrt{2\pi\sigma_m^2}} \frac{\partial}{\partial \mu_m} \exp \left\{ -\frac{(\log(t_i) - \mu_m)^2}{2\sigma_m^2} \right\} \\
&= \frac{\pi_{i,m,g}}{\sum_{j=1}^M \pi_{i,j,g} b_{i,j}} \frac{1}{t_i \sqrt{2\pi\sigma_m^2}} \exp \left\{ -\frac{(\log(t_i) - \mu_m)^2}{2\sigma_m^2} \right\} \frac{\partial}{\partial \mu_m} \left(-\frac{\log(t_i) - \mu_m)^2}{2\sigma_m^2} \right) \\
&= \frac{\pi_{i,m,g} b_{i,m}(t_i) - \mu_m}{\sigma_m^2 f_u(t_i) \mid \mathbf{x}_i, \boldsymbol{\mu}, \boldsymbol{\sigma}}
\end{aligned}$$

The derivative for μ_m is:

$$\begin{aligned}
&\frac{\partial}{\partial \mu_m} l(\boldsymbol{\mu} \mid \mathbf{t}, \boldsymbol{\sigma}, \boldsymbol{\beta}, \boldsymbol{\lambda}_g, \mathbf{x}_i) \\
&= \sum_i \sum_g \frac{\delta_i r_g(\mathbf{x}_i) \pi_{i,m,g} \phi_m(\log(t_i) - \mu_m / \sigma_m)}{\sigma_m S_g(t_i) \mid \boldsymbol{\lambda}_g, \mathbf{x}_i, \boldsymbol{\mu}, \boldsymbol{\sigma}} + \frac{(1 - \delta_i) \pi_{i,m,g} b_{i,m}(t_i) - \mu_m}{\sigma_m^2 f_u(t_i) \mid \mathbf{x}_i, \boldsymbol{\mu}, \boldsymbol{\sigma}} \\
&= \sum_i \sum_g \pi_{i,m,g} \left(\frac{\delta_i r_g(\mathbf{x}_i) \phi_m(\log(t_i) - \mu_m / \sigma_m)}{\sigma_m S_g(t_i) \mid \boldsymbol{\lambda}_g, \mathbf{x}_i, \boldsymbol{\mu}, \boldsymbol{\sigma}} + \frac{(1 - \delta_i) b_{i,m}(t_i) - \mu_m}{\sigma_m^2 f_u(t_i) \mid \mathbf{x}_i, \boldsymbol{\mu}, \boldsymbol{\sigma}} \right)
\end{aligned}$$

S2.1.3 Gradient of $\boldsymbol{\lambda}_g$

The derivative of susceptible probability with respect to the p -th element is

$$\begin{aligned}
\frac{\partial}{\partial \lambda_p} r_g(\mathbf{x}_i) &= c'_g(\mathbf{x}_i) x_p \\
&= r_g(\mathbf{x}_i) (1 - r_g(\mathbf{x}_i)) x_p
\end{aligned}$$

With the likelihood function, notice that we can expand the function as

$$\begin{aligned}
l(\boldsymbol{\lambda}_g \mid \mathbf{t}, \boldsymbol{\pi}, \boldsymbol{\mu}, \boldsymbol{\sigma}, \mathbf{x}_i) &= \sum_{i=1}^N \delta_i \log \left((1 - r_g(\mathbf{x}_i)) + r_g(\mathbf{x}_i) \sum_j \pi_{i,j,g} (1 - a_{i,j}) \right) \\
&\quad + (1 - \delta_i) \log \left(r_g(\mathbf{x}_i) \sum_j \pi_{i,j,g} b_{i,j} \right) \\
&= \sum_{i=1}^N \delta_i \log \left((1 - r_g(\mathbf{x}_i)) + r_g(\mathbf{x}_i) \sum_j \pi_{i,j,g} (1 - a_{i,j}) \right)
\end{aligned}$$

$$+ (1 - \delta_i) \log(r_g(\mathbf{x}_i)) + (1 - \delta_i) \log \left(\sum_j \pi_{i,j,g} b_{i,j} \right),$$

which allows the last term to not be included in the calculation for the gradient.

Then the derivative is as follows

$$\begin{aligned} \frac{\partial}{\partial \lambda_p} l(\boldsymbol{\lambda}_g \mid \mathbf{t}, \boldsymbol{\pi}, \boldsymbol{\mu}, \boldsymbol{\sigma}, \mathbf{x}_i) &= \sum_{i=1}^N \frac{\delta_i (r_g(\mathbf{x}_i) (1 - r_g(\mathbf{x}_i)) x_{i,p})}{S_g(t_i) \mid \boldsymbol{\lambda}_g, \mathbf{x}_i, \boldsymbol{\mu}, \boldsymbol{\sigma}} \left(\sum_j \pi_{i,j,g} (1 - a_{i,j}) - 1 \right) \\ &\quad + \frac{1 - \delta_i}{r_g(\mathbf{x}_i)} r_g(\mathbf{x}_i) (1 - r_g(\mathbf{x}_i)) x_{i,p} \\ &= \sum_{i=1}^N r_g(\mathbf{x}_i) (1 - r_g(\mathbf{x}_i)) x_{i,p} \left[\frac{\delta_i \left(\sum_j \pi_{i,j,g} (1 - a_{i,j}) - 1 \right)}{S_g(t_i) \mid \boldsymbol{\lambda}_g, \mathbf{x}_i, \boldsymbol{\mu}, \boldsymbol{\sigma}} + \frac{1 - \delta_i}{r_g(\mathbf{x}_i)} \right] \end{aligned}$$

S2.2 NN link

The derivative with respect to $\boldsymbol{\beta}_m, \boldsymbol{\lambda}_k, \mu_m$ will remain the same with adjustments to their respective dimensions, if necessary.

The log-likelihood in the nonlinear setting is:

$$\begin{aligned} l(\boldsymbol{\theta} \mid \mathbf{t}, \boldsymbol{\beta}, \boldsymbol{\mu}, \boldsymbol{\sigma}, \boldsymbol{\lambda}_g, \mathbf{x}_i) &= \sum_{i=1}^N \sum_{g=1}^G \delta_i \log \left((1 - r_g(\mathbf{y}_i)) + r_g(\mathbf{y}_i) \sum_m \pi_{i,m,g} (1 - a_{i,m}) \right) \\ &\quad + (1 - \delta_i) \log \left(r_g(\mathbf{y}_i) \sum_m \pi_{i,m,g} b_{i,m} \right) \end{aligned}$$

S2.2.1 Gradient of θ_k

We denote $\mathbf{y}_i = \psi(\mathbf{x}_i^T \boldsymbol{\theta}_k)$, then proceed with the following

$$\begin{aligned} \frac{\partial}{\partial \boldsymbol{\theta}_k} \mathbf{y}_i &= \frac{\partial}{\partial \boldsymbol{\theta}_k} \psi(\mathbf{x}_i^T \boldsymbol{\theta}_k) = \psi'(\mathbf{x}_i^T \boldsymbol{\theta}_k) = \frac{\partial}{\partial \boldsymbol{\theta}_k} \frac{e^{2(\mathbf{x}_i^T \boldsymbol{\theta}_k)} - 1}{e^{2(\mathbf{x}_i^T \boldsymbol{\theta}_k)} + 1} \\ &= \frac{4e^{2(\mathbf{x}_i^T \boldsymbol{\theta}_k)} \mathbf{x}_i}{\left(e^{2(\mathbf{x}_i^T \boldsymbol{\theta}_k)} + 1 \right)^2} \\ \frac{\partial}{\partial \boldsymbol{\theta}_k} r_g(\mathbf{y}_i) &= \boldsymbol{\lambda}_g^T c'(\boldsymbol{\lambda}_g^T \mathbf{y}_i) \psi'(\mathbf{x}_i^T \boldsymbol{\theta}_k) \end{aligned}$$

$$\begin{aligned}
&= \boldsymbol{\lambda}_g^T r_g(\mathbf{y}_i) (1 - r_g(\mathbf{y}_i)) \psi'(\mathbf{x}_i^T \boldsymbol{\theta}_k) \\
\frac{\partial}{\partial \boldsymbol{\theta}_k} \pi_{i,j,g} &= \frac{\partial}{\partial \boldsymbol{\theta}_k} \frac{\gamma_{j,g} \exp(\mathbf{y}_i^T \boldsymbol{\beta}_j)}{\sum_{w=1}^M \gamma_{w,g} \exp(\mathbf{y}_i^T \boldsymbol{\beta}_w)} \\
&= \gamma_{j,g} \exp(\mathbf{y}_i^T \boldsymbol{\beta}_j) \psi'(\mathbf{x}_i^T \boldsymbol{\theta}_k) \left(\frac{\beta_{jk} \sum_w \gamma_{w,g} \exp(\mathbf{y}_i^T \boldsymbol{\beta}_w) - \sum_w \beta_{wk} \gamma_{w,g} \exp(\mathbf{y}_i^T \boldsymbol{\beta}_w)}{\left(\sum_w \gamma_{w,g} \exp(\mathbf{y}_i^T \boldsymbol{\beta}_w) \right)^2} \right) \\
&= \pi_{i,j,g} \psi'(\mathbf{x}_i^T \boldsymbol{\theta}_k) \left(\beta_{jk} - \frac{\sum_w \beta_{wk} \gamma_{w,g} \exp(\mathbf{y}_i^T \boldsymbol{\beta}_w)}{\sum_w \gamma_{w,g} \exp(\mathbf{y}_i^T \boldsymbol{\beta}_w)} \right)
\end{aligned}$$

Then putting it all together:

$$\begin{aligned}
&\frac{\partial}{\partial \boldsymbol{\theta}_k} \delta_i \log \left((1 - r_g(\mathbf{y}_i)) + r_g(\mathbf{y}_i) \sum_m \pi_{i,m,g} (1 - a_{i,m}) \right) \\
&= \frac{\delta_i}{S_g(t_i) \mid \boldsymbol{\lambda}, \mathbf{x}_i, \boldsymbol{\mu}, \boldsymbol{\sigma}} \left(r_g(\mathbf{y}_i) \sum_m \frac{\partial}{\partial \boldsymbol{\theta}_k} \pi_{i,m,g} (1 - a_{i,m}) + \frac{\partial}{\partial \boldsymbol{\theta}_k} r_g(\mathbf{y}_i) \left(\sum_{j=1}^M \pi_{i,j,g} (1 - a_{i,j}) - 1 \right) \right) \\
&= \frac{\delta_i r_g(\mathbf{y}_i)}{S_g(t_i) \mid \boldsymbol{\lambda}, \mathbf{x}_i, \boldsymbol{\mu}, \boldsymbol{\sigma}} \times \\
&\quad \left(\sum_{j=1}^M (1 - a_{i,j}) \frac{\partial}{\partial \boldsymbol{\theta}_k} \pi_{i,j,g} + \lambda_{g,k} \psi'(\mathbf{x}_i^T \boldsymbol{\theta}_k) (1 - r_g(\mathbf{y}_i)) \left(\sum_{j=1}^M \pi_{i,j,g} (1 - a_{i,j}) - 1 \right) \right)
\end{aligned}$$

$$\begin{aligned}
&\frac{\partial}{\partial \boldsymbol{\theta}_k} (1 - \delta_i) \log \left(r_g(\mathbf{y}_i) \sum_m \pi_{i,m,g} b_{i,m} \right) \\
&= \frac{(1 - \delta_i)}{r_g(\mathbf{y}_i) f_u(t_i) \mid \mathbf{x}_i, \boldsymbol{\mu}, \boldsymbol{\sigma}} \left(\frac{\partial}{\partial \boldsymbol{\theta}_k} r_g(\mathbf{y}_i) f_u(t_i) \mid \mathbf{x}_i, \boldsymbol{\mu}, \boldsymbol{\sigma} + r_g(\mathbf{y}_i) \sum_m \frac{\partial}{\partial \boldsymbol{\theta}_k} \pi_{i,m,g} b_{i,m} \right) \\
&= (1 - \delta_i) \left(\lambda_{g,k} \psi'(\mathbf{x}_i^T \boldsymbol{\theta}_k) (1 - r_g(\mathbf{y}_i)) + \frac{1}{f_u(t_i) \mid \mathbf{x}_i, \boldsymbol{\mu}, \boldsymbol{\sigma}} \left(\sum_{j=1}^M b_{i,j} \frac{\partial}{\partial \boldsymbol{\theta}_k} \pi_{i,j,g} \right) \right)
\end{aligned}$$

Then the full expression is:

$$\frac{\partial}{\partial \boldsymbol{\theta}_k} l(\boldsymbol{\theta} \mid \boldsymbol{\mu}, \boldsymbol{\sigma}, \mathbf{t}, \boldsymbol{\lambda}, \mathbf{x}_i) =$$

$$\begin{aligned}
& \sum_{i=1}^N \sum_{g=1}^G \frac{\delta_i r_g(\mathbf{y}_i)}{S_g(t_i) \mid \boldsymbol{\lambda}, \mathbf{x}_i, \boldsymbol{\mu}, \boldsymbol{\sigma}} \times \\
& \left(\sum_{j=1}^M (1 - a_{i,j}) \frac{\partial}{\partial \boldsymbol{\theta}_k} \pi_{i,j,g} + \lambda_{g,k} \psi'(\mathbf{x}_i^T \boldsymbol{\theta}_k) (1 - r_g(\mathbf{y}_i)) \left(\sum_{j=1}^M \pi_{i,j,g} (1 - a_{i,j}) - 1 \right) \right) \\
& + (1 - \delta_i) \left(\lambda_{g,k} \psi'(\mathbf{x}_i^T \boldsymbol{\theta}_k) (1 - r_g(\mathbf{y}_i)) + \frac{1}{f_u(t_i) \mid \mathbf{x}_i, \boldsymbol{\mu}, \boldsymbol{\sigma}} \left(\sum_{j=1}^M b_{i,j} \frac{\partial}{\partial \boldsymbol{\theta}_k} \pi_{i,j,g} \right) \right)
\end{aligned}$$

S3 Bayesian Inference

S3.1 Posterior Sampling

Our sampler iterates between the following steps:

1. **Updating $\boldsymbol{\Gamma}$:** The posterior sampling is given by $\gamma_{m,g} \sim \text{Bernoulli}(\tilde{p}_g)$, where $\tilde{p}_g = \frac{p_g l_g^1}{p_g l_g^1 + (1-p_g) l_g^0}$. To sample $\gamma_{m,g}$, we applied the Gumbel Max-Trick. We can express the log probabilities of the Bernoulli distribution as

$$p_1 = \frac{\exp(x_1)}{\exp(x_1) + \exp(x_2)}, p_2 = \frac{\exp(x_2)}{\exp(x_2) + \exp(x_1)}.$$

In our case, we only need to find the log probability expression for p_g , which can be shown as

$$\tilde{p}_g = \frac{\exp(x_1)}{\exp(x_1) + \exp(x_2)} = \frac{p_g l_g^1}{p_g l_g^1 + (1-p_g) l_g^0},$$

where we can show $x_1 = \log(p_g) + ll_g^1$ and $x_2 = \log(1 - p_g) + ll_g^0$. Here ll_g^1 is the log-likelihood when $\gamma_{m,g} = 1$ and likewise for ll_g^0 . When applying the Gumbel-max trick $y = \underset{i \in \{1,2\}}{\text{argmax}}(x_i + \mathbf{x}_i)$, where $\mathbf{x}_i \sim \text{Gumbel}(0, 1)$ or $-\log(-\log(\text{Unif}(0, 1)))$. The result y gives the index in which value to sample such that if $y = 1$, then $\gamma_{m,g} = 1$, otherwise $\gamma_{m,g} = 0$ for $y = 2$.

We now describe the updates for $(\boldsymbol{\mu}, \boldsymbol{\Lambda}, \boldsymbol{\beta})$, employing the Metropolis-Hastings (MH) sampling algorithm. Specifically, we use the Langevin Monte Carlo (LMC) by utilizing the gradients of the conditional posterior log-likelihood for each parameter of interest. For each parameter, the log-likelihood $\log P(\mathbf{t} \mid \boldsymbol{\mu}, \boldsymbol{\sigma}, \boldsymbol{\beta}, \boldsymbol{\Gamma}, \boldsymbol{\lambda}, \mathbf{x})$ is

$$\sum_{i=1}^N \sum_{g=1}^G \delta_i \log \left((1 - r_g(\mathbf{x}_i)) + r_g(\mathbf{x}_i) \sum_m \pi_{i,m,g} (1 - a_{i,m}) \right) + (1 - \delta_i) \log \left(r_g(\mathbf{x}_i) \sum_m \pi_{i,m,g} b_{i,m} \right).$$

This approach is beneficial for complex hierarchical Bayesian model. We use superscript (t) to represent the corresponding posterior sample at the t -th iteration while describing the MH steps in detail below. For notation, we denote $a_{i,m} = \Phi_m\left(\frac{\log(t_i) - \mu_m}{\sigma_m}\right)$ and $b_{i,m} = \frac{1}{t_i \sqrt{2\pi\sigma_m^2}} \exp\left\{-\frac{(\log(t_i) - \mu_m)^2}{2\sigma_m^2}\right\}$. Furthermore, we can express $S(t_i | \boldsymbol{\Lambda}, \mathbf{x}_i, \boldsymbol{\mu}, \boldsymbol{\sigma}) = (1 - r_g(\mathbf{x}_i)) + r_g(\mathbf{x}_i) \sum_m \pi_{i,m,g} (1 - a_{i,m})$ and $f_{g,u}(\log(t_i) | \mathbf{x}_i, \boldsymbol{\mu}, \boldsymbol{\sigma}) = \sum_m \pi_{i,m,g} b_{i,m}$.

The proposal values for $(\mu_m, \lambda_p, \boldsymbol{\beta}_k)$ are adjusted to achieve a pre-specified acceptance rate, tuning their corresponding ϵ every 200 iterations to maintain an acceptance rate between 0.45 and 0.7.

2. **Updating μ_m :** The conditional posterior log-likelihood and its derivative with respect to μ_m are needed this process. The conditional posterior log-likelihood $\log P(\mu_m | \mathbf{t}, \boldsymbol{\sigma}, \boldsymbol{\beta}, \boldsymbol{\Gamma}, \boldsymbol{\Lambda}, \mathbf{x})$ is $\log P(\mathbf{t} | \mu_m, \boldsymbol{\sigma}, \boldsymbol{\beta}, \boldsymbol{\Gamma}, \boldsymbol{\Lambda}, \mathbf{x}) - \mu_m^2 / 2\sigma_\mu^2$. The corresponding derivative $\nabla \log P(\mu_m | \mathbf{t}, \boldsymbol{\sigma}, \boldsymbol{\beta}, \boldsymbol{\Gamma}, \boldsymbol{\Lambda}, \mathbf{x})$ with respect to μ_m is:

$$\sum_i \sum_g \pi_{i,m,g} \left(\frac{\delta_i r_g(\mathbf{x}_i) \phi_m(\log(t_i) - \mu_m / \sigma_m)}{\sigma_m S_g(t_i | \boldsymbol{\lambda}_g, \mathbf{x}_i, \boldsymbol{\mu}, \boldsymbol{\sigma})} + \frac{(1 - \delta_i) b_{i,m} (\log(t_i) - \mu_m)}{\sigma_m^2 f_{g,u}(t_i | \mathbf{x}_i, \boldsymbol{\mu}, \boldsymbol{\sigma})} \right) - \frac{\mu_m}{\sigma_\mu^2}.$$

Here $\phi_m(\log(t_i) - \mu_m / \sigma_m)$ is the Normal probability density function. With gradient sampling, our proposed value now depends on the derivative, so that $\mu'_m = \mu_m^{(t)} + \frac{\epsilon}{2} \nabla \log P(\mu_m | \mathbf{t}, \boldsymbol{\sigma}, \boldsymbol{\beta}, \boldsymbol{\Gamma}, \boldsymbol{\Lambda}, \mathbf{x}) |_{\mu_m=\mu_m^{(t)}} + \delta$, where $\delta \sim \text{Normal}(0, \epsilon)$. Thus, the transition probability is

$$q(\mu'_m | \mu_m) \propto \exp\left(-\frac{1}{2\epsilon} \left\| \mu'_m - \mu_m - \frac{\epsilon}{2} \nabla \log P(\mu_m | \mathbf{t}, \boldsymbol{\sigma}, \boldsymbol{\beta}, \boldsymbol{\lambda}, \mathbf{x}) \right\|_2^2\right),$$

and then the acceptance probability for our gradient sampler for a proposed value μ'_m is

$$A(\mu_m^{(t)} \rightarrow \mu'_m) = \frac{P(\mu'_m | \mathbf{t}, \boldsymbol{\sigma}, \boldsymbol{\beta}, \boldsymbol{\Gamma}, \boldsymbol{\Lambda}, \mathbf{x}) q(\mu_m^{(t)} | \mu'_m)}{P(\mu_m^{(t)} | \mathbf{t}, \boldsymbol{\sigma}, \boldsymbol{\beta}, \boldsymbol{\Gamma}, \boldsymbol{\Lambda}, \mathbf{x}) q(\mu'_m | \mu_m^{(t)})} \wedge 1.$$

3. **Updating $\boldsymbol{\beta}_m$:** The conditional posterior log-likelihood $\log P(\boldsymbol{\beta}_m | \mathbf{t}, \boldsymbol{\mu}, \boldsymbol{\sigma}, \boldsymbol{\lambda}, \mathbf{x})$ is $\log P(\mathbf{t} | \boldsymbol{\mu}, \boldsymbol{\sigma}, \beta_m, \boldsymbol{\Gamma}, \boldsymbol{\lambda}, \mathbf{x}) - \sum_p \beta_{m,p}^2 / 2\sigma_\beta^2$ with the derivative $\nabla \log P(\boldsymbol{\beta}_m | \mathbf{t}, \boldsymbol{\mu}, \boldsymbol{\sigma}, \boldsymbol{\Gamma}, \boldsymbol{\lambda}, \mathbf{x})$ as

$$\begin{aligned} & \sum_{i=1}^N \sum_{g=1}^G \frac{\delta_i r_g(\mathbf{x}_i)}{S(t_i | \boldsymbol{\lambda}, \mathbf{x}_i, \boldsymbol{\mu}, \boldsymbol{\sigma})} \left((\pi_{i,m,g} \mathbf{x}_i) \left((1 - a_{i,m})(1 - \pi_{i,m,g}) - \sum_{j \neq m}^M (1 - a_{i,j}) \pi_{i,j,g} \right) \right) \\ & + \frac{(1 - \delta_i)}{f_{g,u}(t_i | \mathbf{x}_i, \boldsymbol{\mu}, \boldsymbol{\sigma})} (\pi_{i,m,g} \mathbf{x}_i) \left(b_{i,m} (1 - \pi_{i,m,g}) - \sum_{j \neq m}^M b_{i,j} \pi_{i,j,g} \right) - \frac{\sum_p \beta_{m,p}}{\sigma_\beta^2}. \end{aligned}$$

We then perform a similar updating step adjusting the transition and acceptance probability for the gradient sampler of a proposed β'_m . Although the length of β_m changes in the nonlinear link to of length K , the derivative conveniently remains the same.

4. **Updating λ_g :** The conditional posterior log-likelihood $\log P(\lambda_g \mid \mathbf{t}, \boldsymbol{\mu}, \boldsymbol{\sigma}, \boldsymbol{\beta}, \boldsymbol{\Gamma}, \mathbf{x})$ is $\log P(\mathbf{t} \mid \boldsymbol{\mu}, \boldsymbol{\sigma}, \boldsymbol{\beta}, \boldsymbol{\Gamma}, \lambda_g, \mathbf{x}) - \sum_p \lambda_{g,p}^2 / 2\sigma_\lambda^2$. Then the derivative $\nabla \log P(\lambda_g \mid \mathbf{t}, \boldsymbol{\mu}, \boldsymbol{\sigma}, \boldsymbol{\beta}, \boldsymbol{\Gamma}, \mathbf{x})$ is

$$\sum_{i=1}^N r_g(\mathbf{x}_i) (1 - r_g(\mathbf{x}_i)) x_{i,p} \left[\frac{\delta_i \left(\sum_j \pi_{i,j,g} (1 - a_{i,j}) - 1 \right)}{S(t_i \mid \lambda_g, \mathbf{x}_i, \boldsymbol{\mu}, \boldsymbol{\sigma})} + \frac{1 - \delta_i}{r_g(\mathbf{x}_i)} \right] - \frac{\sum_p \lambda_{g,p}}{\sigma_\lambda^2}.$$

We then perform a similar updating step adjusting the transition and acceptance probability for the gradient sampler of a proposed λ'_g . The derivative of λ_g remains the same in the nonlinear link.

In the case of the nonlinear link, we also update $\boldsymbol{\theta}$ as well using the gradient based sampler. Similar to $(\boldsymbol{\mu}, \boldsymbol{\lambda}, \boldsymbol{\beta})$, the proposal values for $\boldsymbol{\theta}_k$ are adjusted to achieve a pre-specified acceptance rate, tuning their corresponding ϵ every 200 iterations to maintain an acceptance rate between 0.45 and 0.7.

5. **Updating $\boldsymbol{\theta}_k$:** The conditional posterior log-likelihood $\log P(\boldsymbol{\theta}_k \mid \mathbf{t}, \boldsymbol{\mu}, \boldsymbol{\sigma}, \boldsymbol{\lambda}, \boldsymbol{\Gamma}, \mathbf{x})$ is $\log P(\mathbf{t} \mid \boldsymbol{\mu}, \boldsymbol{\sigma}, \boldsymbol{\beta}, \boldsymbol{\Gamma}, \boldsymbol{\lambda}, \boldsymbol{\theta}_k, \mathbf{x}) - \sum_p \theta_{k,p}^2 / 2\sigma_\theta^2$. Its corresponding derivative $\nabla \log P(\boldsymbol{\theta}_k \mid \mathbf{t}, \boldsymbol{\mu}, \boldsymbol{\sigma}, \boldsymbol{\beta}, \boldsymbol{\Gamma}, \boldsymbol{\lambda}, \mathbf{x})$ is

$$\begin{aligned} & \sum_{i=1}^N \sum_{g=1}^G \frac{\delta_i r_g(\mathbf{x}_i)}{S(t_i \mid \boldsymbol{\lambda}, \mathbf{x}_i, \boldsymbol{\mu}, \boldsymbol{\sigma})} \times \\ & \left(\sum_{j=1}^M (1 - a_{i,j}) \frac{\partial}{\partial \boldsymbol{\theta}_k} \pi_{i,j,g} + \lambda_{g,k} \psi'(\mathbf{x}_i^T \boldsymbol{\theta}_k) (1 - r_g(\mathbf{x}_i)) \left(\sum_{j=1}^M \pi_{i,j,g} (1 - a_{i,j}) - 1 \right) \right) \\ & + (1 - \delta_i) \left(\lambda_{g,k} \psi'(\mathbf{x}_i^T \boldsymbol{\theta}_k) (1 - r_g(\mathbf{x}_i)) + \frac{1}{f_{g,u}(t_i \mid \mathbf{x}_i, \boldsymbol{\mu}, \boldsymbol{\sigma})} \left(\sum_{j=1}^M b_{i,j} \frac{\partial}{\partial \boldsymbol{\theta}_k} \pi_{i,j,g} \right) \right). \end{aligned}$$

The transition and acceptance probability for the gradient sampler of a proposed $\boldsymbol{\theta}'_k$ are the same as the steps above.

S4 Expected survival time

Since we are using a cure model, the expected survival time changes given that a patient is cured or not. If the patient is cured, then $\mathbb{E}(T \mid c(f_g^{(cure)}(\mathbf{x}_i)) = 0) = \infty$. If the patient is

still susceptible, then

$$\begin{aligned} E(T \mid c(f_g^{(cure)}(\mathbf{x}_i)) = 1) &= \int_0^\infty t f(t) dt \\ &= - \int_0^\infty t S'_u(t) dt \end{aligned}$$

where

$$\begin{aligned} S_u(\log(t)) &= c_g(\mathbf{x}_i) S_{g,u}(\log(t)) \\ &= c_g(\mathbf{x}_i) \sum_m \pi_m \left(1 - \Phi_m \left(\frac{\log(t) - \mu_m}{\sigma_m} \right) \right), \\ S'(\log(t)) &= \frac{\partial}{\partial t} c_g(\mathbf{x}_i) \sum_m \pi_m \left(1 - \Phi_m \left(\frac{\log(t) - \mu_m}{\sigma_m} \right) \right) \\ &= c_g(\mathbf{x}_i) \sum_m \pi_m \frac{\partial}{\partial t} \left(1 - \Phi_m \left(\frac{\log(t) - \mu_m}{\sigma_m} \right) \right) \\ &= -c_g(\mathbf{x}_i) \sum_m \pi_m \frac{1}{t \sqrt{2\pi\sigma_m^2}} \exp \left\{ -\frac{(\log(t) - \mu_m)^2}{2\sigma_m^2} \right\} \\ &= -c_g(\mathbf{x}_i) \sum_m \pi_m \frac{1}{t\sigma_m} \phi_m \left(\frac{\log(t) - \mu_m}{\sigma_m} \right) \end{aligned}$$

Now we can find the expected survival time for the susceptible patients

$$\begin{aligned} E(T \mid c(f_g^{(cure)}(\mathbf{x}_i)) = 1) &= - \int_0^\infty t S'_u(t) dt \\ &= \int_0^\infty t c_g(\mathbf{x}_i) \sum_m \pi_m \frac{1}{t\sigma_m} \phi_m \left(\frac{\log(t) - \mu_m}{\sigma_m} \right) dt \\ &= c_g(\mathbf{x}_i) \sum_m \pi_m \int_0^\infty t \frac{1}{t\sigma_m} \phi_m \left(\frac{\log(t) - \mu_m}{\sigma_m} \right) dt, \\ &= c_g(\mathbf{x}_i) \sum_m \pi_m \exp \left(\mu_m + \frac{\sigma_m^2}{2} \right) \end{aligned}$$

S4.1 CATE estimation for survival probability

We define a binary outcome using the indicator function $m_g(T) = \mathbf{I}(T > h)$. Then treatment effect on survival probability at horizon h is

$$\tau_{gg'}^{(h)}(\mathbf{x}) = P(T > h \mid \mathbf{X} = \mathbf{x}, G = g) - P(T > h \mid \mathbf{X} = \mathbf{x}, G = g').$$

Similarly, we can do the same for the survival probability to approximate $Q_m(t)$. We draw the samples from the same distribution. Then the Monte Carlo approximation for $P_{(\mu_m, \sigma_m)}(T > h)$ for a given μ_m, σ_m is $\frac{1}{N_{mc}} \sum_{s=1}^{N_{mc}} (T_{m,s} > h)$. Thus the survival probability can be calculated as

$$\mathbb{E}(\mathbf{I}(T > h) \mid \mathbf{X} = \mathbf{x}) \approx 1 - r_g(\mathbf{x}_i) + r_g(\mathbf{x}_i) \sum_m \pi_m \left[\frac{1}{N_{mc}} \sum_{s=1}^{N_{mc}} (T_{m,s} > h) \right].$$

S5 Simulation

S5.1 Well-specified case

Algorithm S1 Linear generation of Survival Time

for $i \leftarrow 1$ **to** N **do**

 Calculate the susceptible probability using the logistic function:

$$c_g(\mathbf{x}_i) \leftarrow \frac{1}{1 + \exp(-\lambda_{g,0} + \sum_{p=1}^P \mathbf{x}_i^T \lambda_{g,p})} + \text{offset}$$

 Draw $B_i \sim \text{Bernoulli}(1 - c_g(\mathbf{x}_i))$

if $B_i = 1$ **then** ▷ Indicates cure (i.e., a very large survival time)

$t'_i \leftarrow 1000$

else

 Sample m from $\{1, \dots, M\}$ with probabilities $\pi_{i,m,g}$

$t'_i \leftarrow \exp(\text{Normal}(\mu_m, \sigma_m))$

end if

 Generate censoring time $C_i \sim \text{Exponential}(0.05)$

 Set maximum follow-up time $h \leftarrow 25$

if $C_i > h$ **then**

$C_i \leftarrow h + \epsilon$ ▷ Here ϵ is some small noise

end if

 Set final observation time $t_i^* \leftarrow \min(t'_i, C_i)$

end for

Table S1: Comparing mean squared errors for survival probability between the proposed methods and Flexible Parametric Cure Models method, based on 50 replications under different settings of $\lambda_{g,p}$. The reported errors are the medians over all replications.

Method	High Cure Rate			Low Cure Rate		
	ζ_{21} MSE	ζ_{31} MSE	ζ_{32} MSE	ζ_{21} MSE	ζ_{31} MSE	ζ_{32} MSE
$\lambda_{g,p} \sim \text{Unif}(-1, 0)$						
MC Linear	3.16	0.28	3.80	11.25	0.71	11.28
MC Nonlinear $K = 4$	3.08	0.21	3.40	11.40	0.84	11.34
MC Nonlinear $K = 6$	3.18	0.21	3.42	10.72	0.71	11.66
MC Nonlinear $K = 8$	3.11	0.21	3.46	10.71	0.90	11.42
MC Nonlinear $K = 13$	3.05	0.25	3.40	10.92	0.87	11.73
MC Nonlinear $K = 18$	3.02	0.28	3.48	11.74	1.10	11.78
MC Nonlinear $K = K_{CV}$	3.19	0.18	3.55	11.13	0.70	11.84
flexsurvcure (S)	28.65	8.03	23.37	57.93	11.44	62.47
$\lambda_{g,p} \sim \text{Unif}(-2, -1)$						
MC Linear	0.57	0.13	0.53	6.26	0.37	8.81
MC Nonlinear $K = 4$	0.51	0.08	0.41	6.42	0.39	8.66
MC Nonlinear $K = 6$	0.56	0.12	0.47	6.48	0.32	8.67
MC Nonlinear $K = 8$	0.47	0.12	0.46	6.49	0.38	9.30
MC Nonlinear $K = 13$	0.55	0.10	0.47	6.35	0.35	8.93
MC Nonlinear $K = 18$	0.56	0.10	0.45	6.41	0.40	9.22
MC Nonlinear $K = K_{CV}$	0.51	0.10	0.43	6.48	0.45	8.54
flexsurvcure (S)	8.99	5.06	16.39	37.31	14.20	46.62
$\lambda_{g,p} \sim \text{Unif}(-2, 0)$						
MC Linear	1.87	0.20	1.62	8.87	0.47	10.35
MC Nonlinear $K = 4$	1.74	0.22	1.61	9.13	0.44	10.31
MC Nonlinear $K = 6$	1.97	0.24	1.58	8.64	0.53	9.43
MC Nonlinear $K = 8$	1.83	0.24	1.54	8.65	0.55	10.47
MC Nonlinear $K = 13$	1.86	0.21	1.60	8.80	0.55	9.77
MC Nonlinear $K = 18$	1.81	0.23	1.60	8.37	0.71	9.70
MC Nonlinear $K = K_{CV}$	1.86	0.24	1.58	8.93	0.51	9.54
flexsurvcure (S)	13.58	7.70	15.41	52.07	17.48	40.88

Table S2: Comparing mean squared errors for RMST between the proposed methods and Flexible Parametric Cure Models method, based on 50 replications under different settings of $\lambda_{g,p}$. The reported errors are the medians over all replications.

Method	High Cure Rate			Low Cure Rate		
	ζ_{21} MSE	ζ_{31} MSE	ζ_{32} MSE	ζ_{21} MSE	ζ_{31} MSE	ζ_{32} MSE
$\lambda_{g,p} \sim \text{Unif}(-1, 0)$						
MC Linear	5.06	0.90	4.73	20.50	2.09	20.66
MC Nonlinear $K = 4$	4.88	0.87	4.73	20.09	2.34	21.17
MC Nonlinear $K = 6$	5.14	0.87	4.92	20.04	2.09	20.74
MC Nonlinear $K = 8$	5.09	0.78	4.57	20.14	1.98	21.14
MC Nonlinear $K = 13$	5.06	0.85	4.78	20.88	2.19	21.48
MC Nonlinear $K = 18$	5.22	1.01	4.86	20.37	2.35	20.68
MC Nonlinear $K = K_{CV}$	5.18	0.85	4.53	20.14	2.36	21.24
flexsurvcure (S)	14.47	2.21	12.29	54.51	4.24	48.88
$\lambda_{g,p} \sim \text{Unif}(-2, -1)$						
MC Linear	0.82	0.32	0.90	10.73	0.94	9.11
MC Nonlinear $K = 4$	0.81	0.29	0.98	9.94	0.78	9.01
MC Nonlinear $K = 6$	0.78	0.31	0.94	10.35	0.89	8.98
MC Nonlinear $K = 8$	0.77	0.33	0.90	10.45	1.04	9.05
MC Nonlinear $K = 13$	0.78	0.29	0.80	9.95	0.99	9.00
MC Nonlinear $K = 18$	0.77	0.30	0.93	10.38	0.94	9.05
MC Nonlinear $K = K_{CV}$	0.78	0.30	0.95	10.34	0.96	9.08
flexsurvcure (S)	1.97	1.18	3.47	28.09	3.76	30.52

S5.2 Mis-specified case

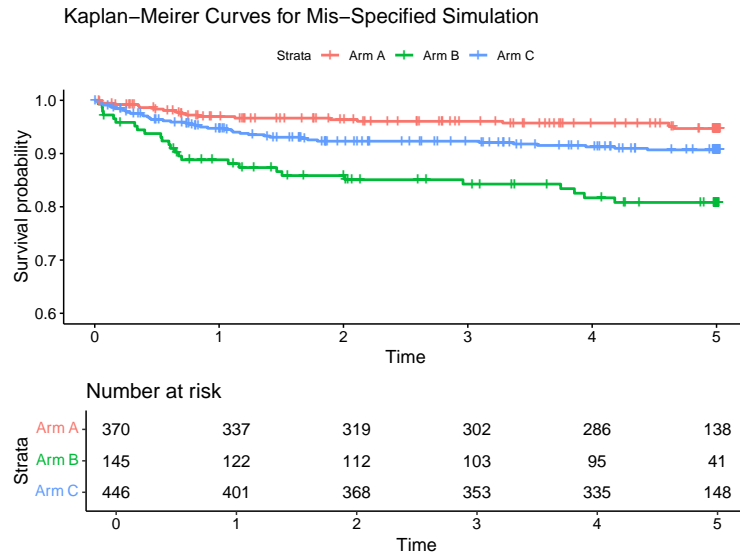


Figure S1: Disease free survival (DFS) Kaplan–Meier curve estimation of the treatment arms for the mis-specified simulation.

Table S3: Comparing mean squared errors for survival probability between the proposed methods and Flexible Parametric Cure Models method, based on 50 replications under different settings of $\lambda_{g,p}$ for misspecified data generation. The reported errors are the medians over all replications.

Method	High Cure Rate			Low Cure Rate		
	ζ_{21} MSE	ζ_{31} MSE	ζ_{32} MSE	ζ_{21} MSE	ζ_{31} MSE	ζ_{32} MSE
$\lambda_{g,p} \sim \text{Unif}(-1, 0)$						
MC Linear	4.14	2.93	3.64	7.37	6.54	8.39
MC Nonlinear $K = 4$	3.53	3.06	3.80	9.08	5.50	9.31
MC Nonlinear $K = 6$	4.44	3.46	3.92	8.50	6.90	9.17
MC Nonlinear $K = 8$	3.69	3.30	3.61	8.86	6.70	9.64
MC Nonlinear $K = 13$	4.01	3.40	3.90	9.20	7.61	10.03
MC Nonlinear $K = 18$	4.53	3.84	3.99	9.71	8.12	10.48
MC Nonlinear $K = K_{CV}$	4.63	3.24	3.81	7.32	6.21	9.83
flexsurvcure (S)	11.54	7.63	9.45	15.80	16.35	14.60
$\lambda_{g,p} \sim \text{Unif}(-2, -1)$						
MC Linear	4.39	3.42	3.08	4.22	6.93	5.17
MC Nonlinear $K = 4$	4.42	4.38	3.01	5.84	7.63	6.32
MC Nonlinear $K = 6$	4.98	4.53	3.32	5.48	7.57	6.21
MC Nonlinear $K = 8$	5.28	4.34	3.43	6.35	7.92	6.89
MC Nonlinear $K = 13$	4.51	5.06	3.56	6.73	8.54	6.64
MC Nonlinear $K = 18$	5.28	5.39	3.61	7.30	9.74	7.81
MC Nonlinear $K = K_{CV}$	4.98	4.57	3.08	6.80	7.58	6.07
flexsurvcure (S)	4.31	5.97	9.34	12.34	15.92	11.32
$\lambda_{g,p} \sim \text{Unif}(-2, 0)$						
MC Linear	4.58	3.96	3.25	4.49	7.43	5.94
MC Nonlinear $K = 4$	4.68	4.84	2.96	6.10	8.42	6.65
MC Nonlinear $K = 6$	5.48	4.65	3.59	5.28	9.54	6.80
MC Nonlinear $K = 8$	5.45	4.21	3.70	5.72	9.38	7.41
MC Nonlinear $K = 13$	5.24	5.06	3.52	6.43	9.72	7.54
MC Nonlinear $K = 18$	5.83	5.68	3.71	7.71	10.96	9.05
MC Nonlinear $K = K_{CV}$	4.92	4.55	3.81	5.32	9.19	6.63
flexsurvcure (S)	9.40	13.17	11.45	12.07	16.72	17.81

Table S4: Comparing mean squared errors for RMST between the proposed methods and Flexible Parametric Cure Models method, based on 50 replications under different settings of $\lambda_{g,p}$ for nonlinear data generation. The reported errors are the medians over all replications.

	High Cure Rate			Low Cure Rate		
	ζ_{21} MSE	ζ_{31} MSE	ζ_{32} MSE	ζ_{21} MSE	ζ_{31} MSE	ζ_{32} MSE
Unif(-1, 0)						
MC Linear	3.49	3.81	6.34	9.97	9.90	15.70
MC Nonlinear $K = 4$	3.51	2.91	4.99	9.02	7.89	15.70
MC Nonlinear $K = 6$	3.71	3.66	6.54	9.86	8.13	16.16
MC Nonlinear $K = 8$	3.96	3.51	5.51	9.66	8.31	14.66
MC Nonlinear $K = 13$	5.34	3.29	5.86	10.50	9.60	17.17
MC Nonlinear $K = 18$	3.71	3.44	5.89	9.62	10.60	16.48
MC Nonlinear $K = K_{CV}$	3.55	3.75	5.34	10.05	8.31	15.74
flexsurvcure (S)	13.01	9.02	12.00	22.36	23.68	19.40
Unif(-2, -1)						
MC Linear	4.25	5.20	6.14	5.89	5.61	9.58
MC Nonlinear $K = 4$	4.09	4.37	4.80	6.08	5.47	7.96
MC Nonlinear $K = 6$	3.38	2.43	6.24	6.15	6.12	8.71
MC Nonlinear $K = 8$	3.93	3.69	6.00	6.79	5.91	9.48
MC Nonlinear $K = 13$	3.85	4.10	8.92	7.16	6.51	10.24
MC Nonlinear $K = 18$	4.97	4.52	11.54	8.16	7.08	10.27
MC Nonlinear $K = K_{CV}$	4.87	5.08	6.24	6.52	5.93	8.76
flexsurvcure (S)	5.30	6.44	11.68	16.89	19.63	16.27

Table S5: Comparison of thresholding-based $s_{p,t}$ -values for $\widehat{\zeta}_{31}$, $\widehat{\zeta}_{21}$, and $\widehat{\zeta}_{32}$ for different choices of thresholds (t), and predictors in different cure rate setting for $N = 961$. The thresholding levels are given in the first column. The generated outcomes are independent of the CNS Status predictor, shown in italics. The exclusion proportions are based on 50 replicated datasets.

$\widehat{\zeta}_{21}$	High Cure Rate				Low Cure Rate			
	Age	WBC	Sex	<i>CNS Status</i>	Age	WBC	Sex	<i>CNS Status</i>
0.00	1.00	1.00	1.00	1.00	1.00	1.00	1.00	1.00
0.05	0.43	0.45	0.23	0.24	0.60	0.61	0.36	0.31
0.10	0.25	0.26	0.13	0.12	0.37	0.39	0.19	0.14
0.15	0.17	0.17	0.10	0.08	0.24	0.26	0.14	0.09
0.20	0.12	0.12	0.08	0.06	0.17	0.20	0.12	0.06
0.25	0.09	0.08	0.07	0.04	0.12	0.17	0.11	0.05
0.30	0.07	0.06	0.05	0.03	0.09	0.14	0.10	0.04
0.35	0.06	0.05	0.04	0.02	0.07	0.13	0.09	0.03
0.40	0.05	0.04	0.04	0.02	0.06	0.11	0.08	0.02
<hr/>								
$\widehat{\zeta}_{31}$								
0.00	1.00	1.00	1.00	1.00	1.00	1.00	1.00	1.00
0.05	0.40	0.39	0.22	0.23	0.65	0.70	0.41	0.40
0.10	0.22	0.21	0.14	0.11	0.42	0.48	0.22	0.21
0.15	0.15	0.14	0.11	0.07	0.29	0.35	0.18	0.14
0.20	0.10	0.10	0.09	0.05	0.20	0.27	0.16	0.10
0.25	0.08	0.07	0.08	0.03	0.15	0.23	0.15	0.08
0.30	0.06	0.05	0.07	0.02	0.11	0.20	0.14	0.06
0.35	0.05	0.04	0.06	0.02	0.09	0.19	0.13	0.05
0.40	0.04	0.03	0.05	0.01	0.08	0.17	0.12	0.04
<hr/>								
$\widehat{\zeta}_{32}$								
0.00	1.00	1.00	1.00	1.00	1.00	1.00	1.00	1.00
0.05	0.45	0.44	0.24	0.22	0.54	0.57	0.31	0.29
0.10	0.24	0.23	0.13	0.10	0.33	0.35	0.17	0.15
0.15	0.15	0.14	0.09	0.07	0.23	0.24	0.14	0.10
0.20	0.10	0.10	0.07	0.05	0.16	0.19	0.12	0.08
0.25	0.07	0.07	0.06	0.03	0.12	0.16	0.11	0.06
0.30	0.05	0.05	0.05	0.03	0.09	0.14	0.09	0.05
0.35	0.04	0.04	0.04	0.02	0.07	0.13	0.08	0.04
0.40	0.03	0.03	0.03	0.01	0.06	0.12	0.07	0.03

Table S6: Comparison of MBLP data partition thresholding-based $s_{p,t}$ -values for $\widehat{\boldsymbol{\zeta}}_{31}$, $\widehat{\boldsymbol{\zeta}}_{21}$, and $\widehat{\boldsymbol{\zeta}}_{32}$ for different clusters and predictors in low cure rate setting for $N = 961$. The thresholding levels are given in the first column. The generated outcomes are independent of the CNS Status predictor. The exclusion proportions are based on 50 replicated datasets.

	$\boldsymbol{\zeta}_{21}$				$\boldsymbol{\zeta}_{31}$				$\boldsymbol{\zeta}_{32}$			
	Age WBC Sex CNS Status				Age WBC Sex CNS Status				Age WBC Sex CNS Status			
	Cluster 1											
0.00	1.00	1.00	1.00	1.00	1.00	1.00	1.00	1.00	1.00	1.00	1.00	1.00
0.05	0.83	0.80	0.57	0.54	0.88	0.84	0.67	0.67	0.82	0.77	0.56	0.52
0.10	0.70	0.65	0.36	0.33	0.77	0.71	0.44	0.46	0.66	0.61	0.33	0.32
0.15	0.58	0.53	0.24	0.21	0.67	0.60	0.31	0.33	0.54	0.50	0.22	0.20
0.20	0.49	0.44	0.18	0.14	0.58	0.52	0.24	0.24	0.45	0.42	0.16	0.14
0.25	0.42	0.38	0.13	0.10	0.50	0.45	0.19	0.17	0.38	0.35	0.13	0.10
0.30	0.36	0.33	0.10	0.07	0.44	0.40	0.16	0.12	0.32	0.30	0.10	0.08
0.35	0.30	0.29	0.08	0.05	0.38	0.36	0.13	0.09	0.27	0.26	0.08	0.06
0.40	0.26	0.25	0.07	0.04	0.33	0.32	0.11	0.06	0.23	0.23	0.07	0.04
	Cluster 2											
0.00	1.00	1.00	1.00	1.00	1.00	1.00	1.00	1.00	1.00	1.00	1.00	1.00
0.05	0.83	0.83	0.60	0.61	0.87	0.88	0.69	0.65	0.81	0.80	0.56	0.54
0.10	0.70	0.68	0.38	0.39	0.77	0.76	0.46	0.43	0.67	0.65	0.35	0.29
0.15	0.60	0.57	0.27	0.25	0.68	0.66	0.34	0.27	0.56	0.53	0.25	0.17
0.20	0.52	0.47	0.21	0.16	0.60	0.56	0.27	0.18	0.47	0.45	0.19	0.11
0.25	0.45	0.40	0.18	0.11	0.54	0.48	0.24	0.12	0.41	0.38	0.15	0.07
0.30	0.39	0.34	0.15	0.08	0.48	0.41	0.21	0.09	0.35	0.33	0.12	0.05
0.35	0.34	0.30	0.13	0.06	0.42	0.36	0.19	0.07	0.31	0.29	0.11	0.04
0.40	0.30	0.26	0.12	0.04	0.38	0.32	0.17	0.05	0.27	0.26	0.09	0.03
	Cluster 3											
0.00	1.00	1.00	1.00	1.00	1.00	1.00	1.00	1.00	1.00	1.00	1.00	1.00
0.05	0.81	0.83	0.65	0.51	0.84	0.88	0.69	0.61	0.78	0.80	0.56	0.48
0.10	0.66	0.71	0.45	0.28	0.70	0.77	0.48	0.36	0.62	0.66	0.35	0.26
0.15	0.55	0.61	0.33	0.18	0.60	0.68	0.34	0.21	0.50	0.55	0.24	0.15
0.20	0.46	0.53	0.24	0.12	0.51	0.60	0.25	0.13	0.42	0.47	0.18	0.09
0.25	0.39	0.46	0.19	0.08	0.44	0.53	0.19	0.08	0.35	0.41	0.14	0.06
0.30	0.33	0.41	0.15	0.06	0.38	0.48	0.15	0.06	0.29	0.36	0.11	0.04
0.35	0.29	0.36	0.12	0.05	0.33	0.43	0.12	0.04	0.25	0.32	0.09	0.03
0.40	0.25	0.33	0.10	0.04	0.29	0.40	0.10	0.03	0.22	0.29	0.08	0.02
	Cluster 4											
0.00	1.00	1.00	1.00	1.00	1.00	1.00	1.00	1.00	1.00	1.00	1.00	1.00
0.05	0.82	0.81	0.62	0.63	0.87	0.86	0.69	0.73	0.80	0.80	0.56	0.57
0.10	0.69	0.67	0.40	0.39	0.76	0.74	0.47	0.53	0.66	0.65	0.33	0.34
0.15	0.59	0.57	0.26	0.24	0.66	0.65	0.32	0.38	0.55	0.55	0.21	0.21
0.20	0.50	0.48	0.17	0.15	0.58	0.58	0.22	0.27	0.46	0.47	0.15	0.14
0.25	0.44	0.42	0.12	0.09	0.51	0.52	0.16	0.19	0.40	0.41	0.11	0.10
0.30	0.38	0.37	0.09	0.06	0.46	0.47	0.12	0.13	0.34	0.36	0.08	0.07
0.35	0.33	0.32	0.06	0.04	0.41	0.42	0.10	0.09	0.30	0.32	0.07	0.05
0.40	0.30	0.29	0.05	0.03	0.37	0.38	0.08	0.07	0.27	0.28	0.05	0.04

Algorithm S2 Non-linear generation of Survival Time**for** $i \leftarrow 1$ **to** N **do**

Calculate the susceptible probability using the logistic function:

$$c_g(\mathbf{x}_i) \leftarrow \frac{1}{1 + \exp(-\lambda_{g,0} + \sum_{p=1}^P \mathbf{x}_i^T \lambda_{g,p})} + \text{offset}_g$$

Sample m from $\{1, \dots, M\}$ with probabilities $\pi_{i,m,g}$ Draw $B_i \sim \text{Bernoulli}(1 - c_g(\mathbf{x}_i))$ **if** $B_i = 1$ **then** ▷ Indicates cure (i.e., a very large survival time)

$t'_i \leftarrow 1000$

else

$t'_i \leftarrow \exp(\text{Normal}(\mu_{i,m}, \sigma_m^2))$

end ifGenerate censoring time $C_i \sim \text{Exponential}(0.05)$ Set maximum follow-up time $h \leftarrow 5$ **if** $C_i > h$ **then**

$C_i \leftarrow h + \epsilon$

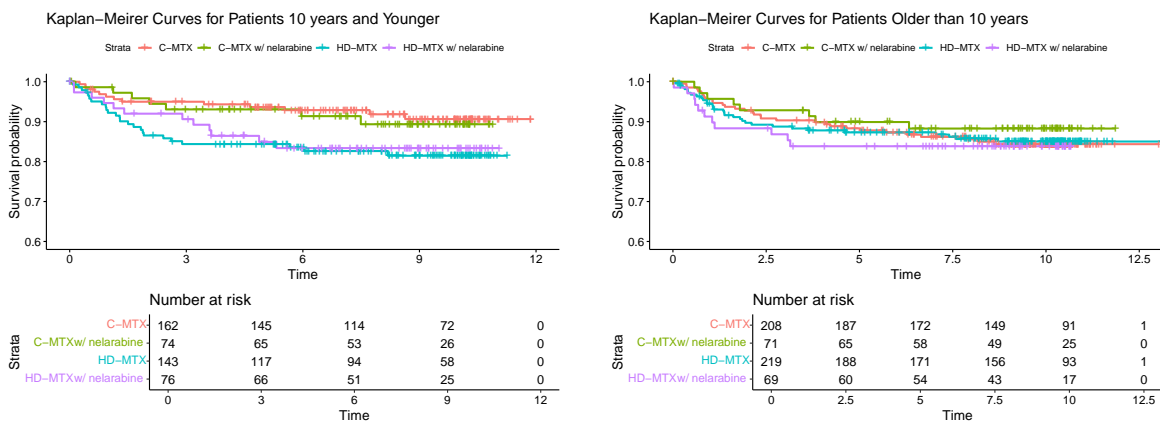
▷ Here ϵ is some small noise**end if**Set final observation time $t_i^* \leftarrow \min(t'_i, C_i)$ **end for****S6. Additional Figures and Tables from AALL0434 Data Analysis**

Figure S2: Estimated survival curves for patients based on age

Table S7: Comparison of thresholding-based $s_{p,t}$ -values for $\hat{\zeta}_{41}$, $\hat{\zeta}_{32}$, and $\hat{\zeta}_{42}$ for different choices of thresholds (t), and predictors for the AALL0434 dataset.

	Age	CNS Status	Sex	WBC Count	Risk Status 2	Risk Status 3
Threshold	$\hat{\zeta}_{41}$					
0.00	1.00	1.00	1.00	1.00	1.00	1.00
0.05	0.95	0.89	0.91	0.97	0.90	0.90
0.10	0.91	0.79	0.82	0.91	0.81	0.81
0.15	0.88	0.70	0.75	0.86	0.72	0.75
0.20	0.82	0.64	0.68	0.82	0.67	0.69
0.25	0.78	0.57	0.62	0.80	0.62	0.63
0.30	0.74	0.51	0.58	0.77	0.55	0.58
0.35	0.70	0.45	0.54	0.73	0.51	0.54
0.40	0.65	0.41	0.51	0.70	0.46	0.50
	$\hat{\zeta}_{32}$					
0.00	1.00	1.00	1.00	1.00	1.00	1.00
0.05	0.96	0.87	0.91	0.95	0.90	0.91
0.10	0.89	0.75	0.81	0.90	0.82	0.83
0.15	0.82	0.66	0.73	0.87	0.74	0.76
0.20	0.77	0.58	0.66	0.81	0.67	0.69
0.25	0.71	0.52	0.59	0.77	0.60	0.63
0.30	0.66	0.47	0.52	0.74	0.53	0.57
0.35	0.60	0.42	0.46	0.70	0.48	0.54
0.40	0.55	0.37	0.42	0.67	0.44	0.50
	$\hat{\zeta}_{42}$					
0.00	1.00	1.00	1.00	1.00	1.00	1.00
0.05	0.93	0.88	0.90	0.94	0.91	0.90
0.10	0.86	0.76	0.82	0.89	0.81	0.81
0.15	0.80	0.67	0.74	0.84	0.74	0.74
0.20	0.73	0.60	0.67	0.80	0.68	0.68
0.25	0.67	0.54	0.61	0.76	0.61	0.63
0.30	0.62	0.49	0.56	0.72	0.56	0.57
0.35	0.57	0.43	0.52	0.69	0.51	0.53
0.40	0.54	0.37	0.48	0.66	0.47	0.49

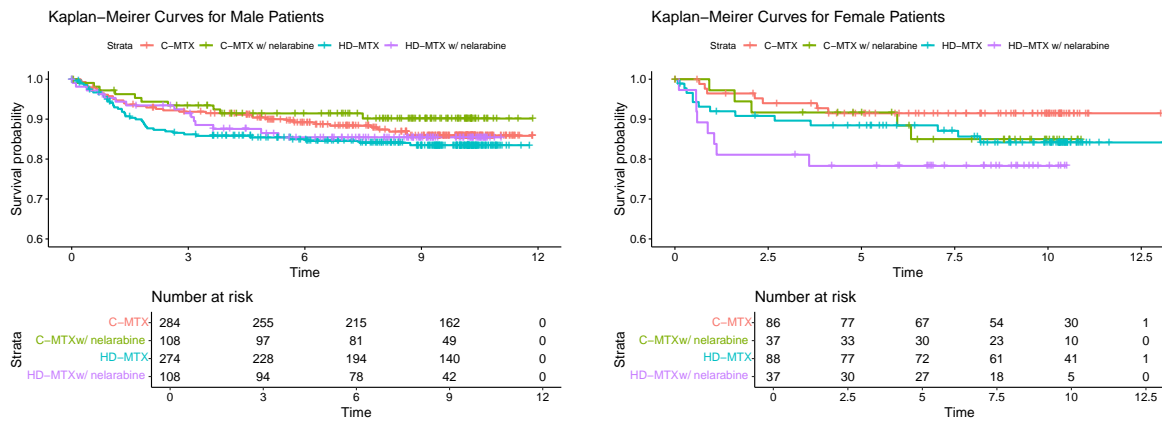


Figure S3: Estimated survival curves for patients based on sex

Table S8: Comparison of BLP data partition thresholding-based $s_{p,t}$ -values for $\widehat{\zeta}_{41}$, $\widehat{\zeta}_{32}$, and $\widehat{\zeta}_{42}$ for different clusters and predictors for the AALL0434 dataset. The thresholding levels are given in the first column.

		Cluster 1					
		Age	CNS Status	Sex	WBC Count	Risk Status 2	Risk Status 3
Threshold		$\widehat{\zeta}_{41}$					
0.00	1.00	1.00	1.00	1.00	1.00	1.00	
0.05	0.93	0.90	0.90	0.97	0.92	0.91	
0.10	0.87	0.80	0.81	0.94	0.83	0.83	
0.15	0.79	0.71	0.75	0.91	0.75	0.76	
0.20	0.72	0.64	0.66	0.88	0.69	0.69	
0.25	0.66	0.57	0.61	0.84	0.62	0.64	
0.30	0.62	0.51	0.56	0.80	0.55	0.59	
0.35	0.58	0.46	0.53	0.77	0.50	0.54	
0.40	0.54	0.41	0.49	0.74	0.43	0.49	
		$\widehat{\zeta}_{32}$					
0.00	1.00	1.00	1.00	1.00	1.00	1.00	
0.05	0.94	0.88	0.91	0.96	0.93	0.93	
0.10	0.87	0.78	0.81	0.93	0.84	0.86	
0.15	0.82	0.68	0.74	0.90	0.77	0.79	
0.20	0.76	0.61	0.65	0.86	0.70	0.73	
0.25	0.71	0.54	0.58	0.81	0.64	0.68	
0.30	0.65	0.49	0.51	0.77	0.58	0.62	
0.35	0.61	0.44	0.45	0.72	0.53	0.57	
0.40	0.56	0.40	0.41	0.69	0.47	0.52	
		$\widehat{\zeta}_{42}$					
0.00	1.00	1.00	1.00	1.00	1.00	1.00	
0.05	0.93	0.89	0.90	0.95	0.93	0.91	
0.10	0.86	0.80	0.81	0.91	0.84	0.84	
0.15	0.80	0.69	0.74	0.87	0.76	0.78	
0.20	0.73	0.60	0.66	0.82	0.69	0.70	
0.25	0.67	0.53	0.61	0.77	0.64	0.64	
0.30	0.62	0.48	0.57	0.73	0.60	0.57	
0.35	0.58	0.42	0.51	0.70	0.54	0.53	
0.40	0.52	0.38	0.47	0.67	0.49	0.50	
		Cluster 2					
		$\widehat{\zeta}_{41}$					
0.00	1.00	1.00	1.00	1.00	1.00	1.00	
0.05	0.97	0.92	0.91	0.97	0.93	0.91	
0.10	0.93	0.83	0.83	0.94	0.85	0.83	
0.15	0.89	0.74	0.77	0.91	0.77	0.76	
0.20	0.84	0.65	0.71	0.87	0.70	0.70	
0.25	0.81	0.59	0.63	0.84	0.64	0.63	
0.30	0.76	0.53	0.59	0.81	0.59	0.59	
0.35	0.71	0.48	0.56	0.78	0.54	0.55	
0.40	0.68	0.42	0.51	0.74	0.50	0.51	
		$\widehat{\zeta}_{32}$					
0.00	1.00	1.00	1.00	1.00	1.00	1.00	
0.05	0.94	0.88	0.92	0.97	0.92	0.92	
0.10	0.88	0.77	0.82	0.92	0.82	0.84	
0.15	0.83	0.69	0.74	0.88	0.75	0.77	
0.20	0.78	0.61	0.68	0.84	0.68	0.70	
0.25	0.72	0.55	0.60	0.81	0.61	0.64	
0.30	0.67	0.49	0.54	0.78	0.55	0.59	
0.35	0.62	0.44	0.47	0.74	0.51	0.55	
0.40	0.56	0.39	0.42	0.71	0.46	0.51	
		$\widehat{\zeta}_{42}$					
0.00	1.00	1.00	1.00	1.00	1.00	1.00	
0.05	0.94	0.87	0.90	0.97	0.91	0.90	
0.10	0.87	0.75	0.81	0.92	0.82	0.81	
0.15	0.80	0.68	0.72	0.88	0.76	0.75	
0.20	0.76	0.61	0.66	0.84	0.70	0.69	
0.25	0.70	0.56	0.62	0.80	0.64	0.63	
0.30	0.65	0.50	0.57	0.77	0.58	0.58	
0.35	0.59	0.45	0.53	0.74	0.53	0.54	
0.40	0.55	0.40	0.49	0.70	0.48	0.49	

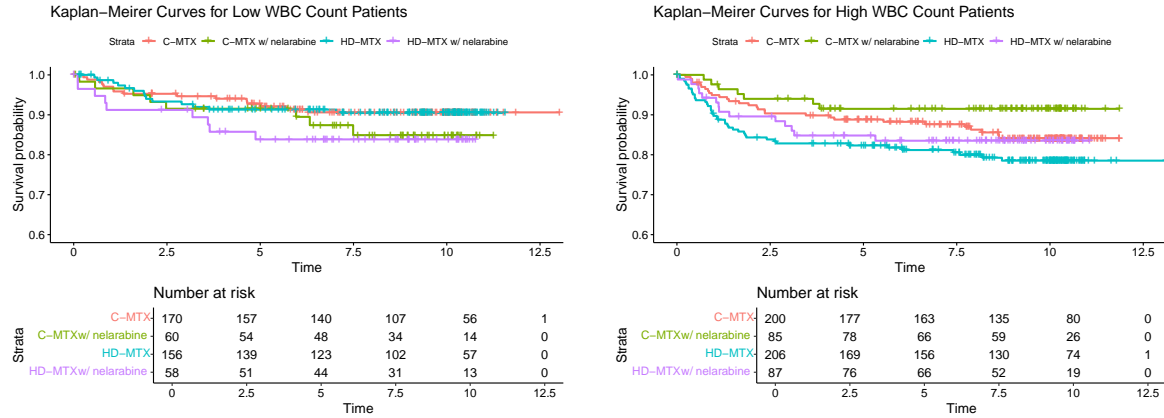


Figure S4: Estimated survival curves for both high and low WBC count patients, here high WBC count is considered having a count of at least $50,000 \mu\text{L}$.

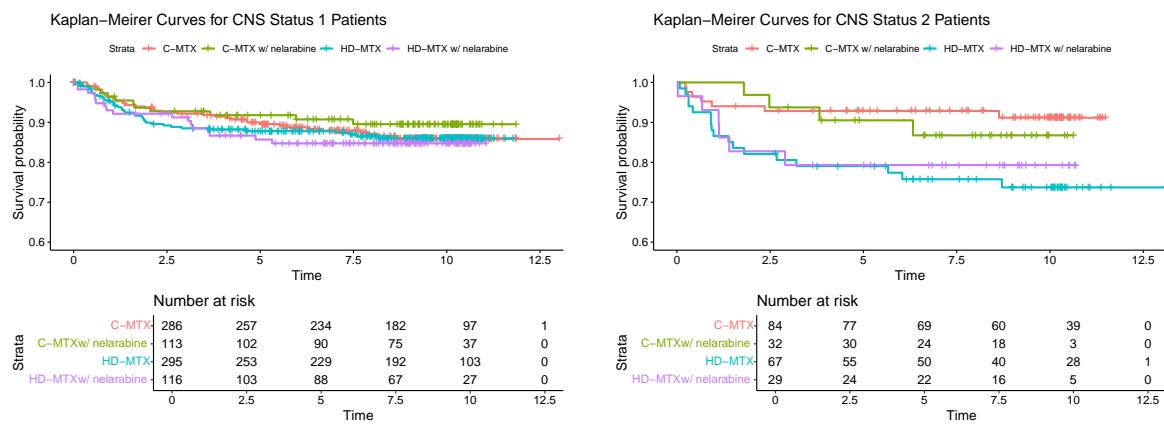


Figure S5: Estimated survival curves for patients with different CNS status

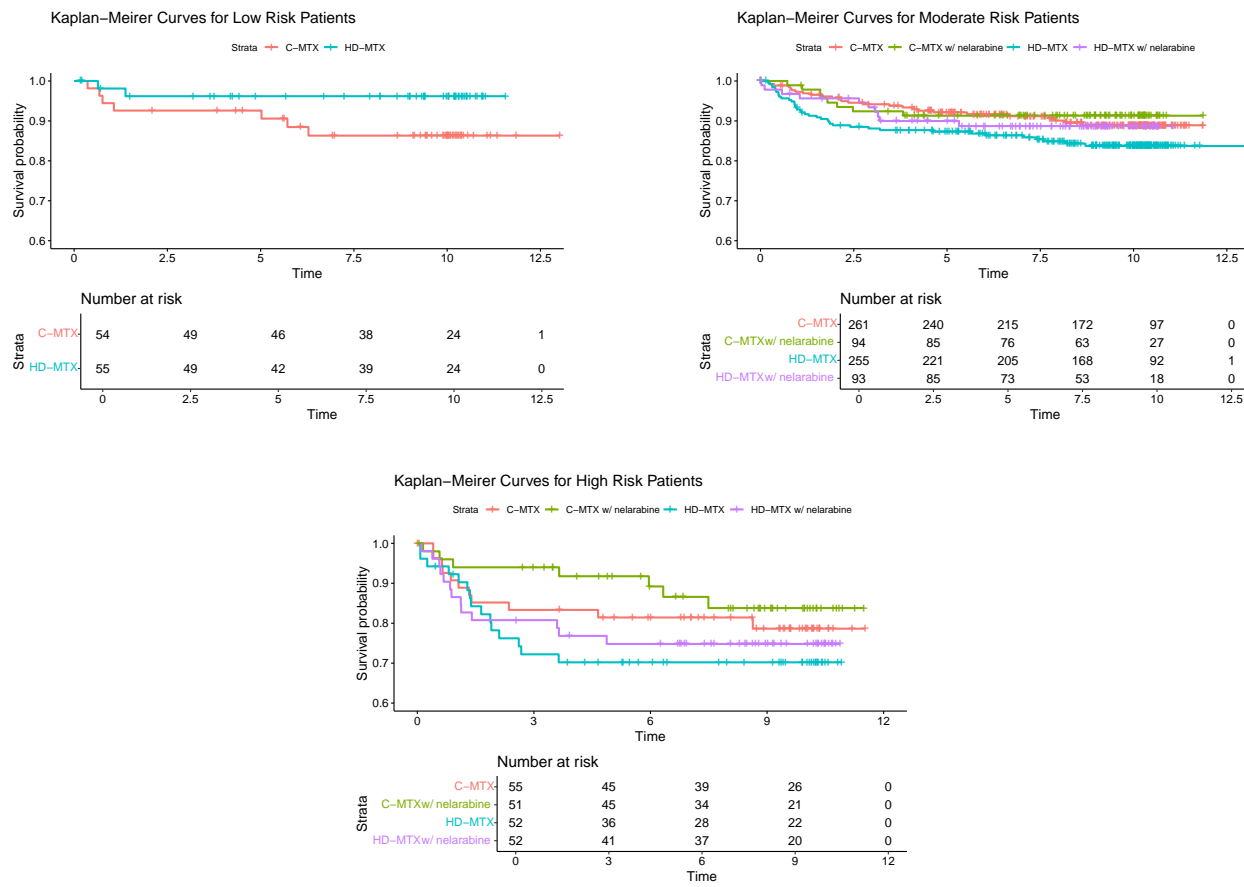


Figure S6: Estimated survival curves for patients based on Risk Status

References

Amdahl, J. (2022), *flexsurvcure: Flexible Parametric Cure Models*. R package version 1.3.1.

Anastassiou, G. A. (2011), “Multivariate hyperbolic tangent neural network approximation,” *Computers & Mathematics with Applications*, 61(4), 809–821.

Berkson, J., and Gage, R. P. (1952), “Survival curve for cancer patients following treatment,” *Journal of the American Statistical Association*, 47(259), 501–515.

Bishop, C. M., and Svensén, M. (2003), Bayesian hierarchical mixtures of experts,, in *Uncertainty in Artificial Intelligence: Proceedings of the Nineteenth Conference*, pp. 57–64.

Boag, J. W. (1949), “Maximum likelihood estimates of the proportion of patients cured by cancer therapy,” *Journal of the Royal Statistical Society. Series B (Methodological)*, 11(1), 15–53.

Cai, C., Zou, Y., Peng, Y., and Zhang, J. (2012), “smcure: An R-Package for estimating semiparametric mixture cure models,” *Computer methods and programs in biomedicine*, 108(3), 1255–1260.

Chang, P., and Roy, A. (2025), “Individualized multi-treatment response curves estimation using RBF-net with shared neurons,” *Biometrics*, 81(1), ujaf019.

Cui, Y., Kosorok, M. R., Sverdrup, E., Wager, S., and Zhu, R. (2023), “Estimating heterogeneous treatment effects with right-censored data via causal survival forests,” *Journal of the Royal Statistical Society Series B: Statistical Methodology*, 85(2), 179–211.

Cybenko, G. (1989), “Approximation by superpositions of a sigmoidal function,” *Mathematics of control, signals and systems*, 2(4), 303–314.

De la Cruz, R., Fuentes, C., and Padilla, O. (2022), “A Bayesian mixture cure rate model for estimating short-term and long-term recidivism,” *Entropy*, 25(1), 56.

Dunsmore, K. P., Winter, S. S., Devidas, M., Wood, B. L., Esiashvili, N., Chen, Z., Eisenberg, N., Biegel, N., Hayashi, R. J., Gastier-Foster, J. M. et al. (2020), “Children’s Oncology Group AALL0434: a phase III randomized clinical trial testing nelarabine in newly diagnosed T-cell acute lymphoblastic leukemia,” *Journal of Clinical Oncology*, 38(28), 3282–3293.

Farewell, V. T. (1982), “The use of mixture models for the analysis of survival data with long-term survivors,” *Biometrics*, pp. 1041–1046.

Hanin, L., and Huang, L.-S. (2014), “Identifiability of cure models revisited,” *Journal of Multivariate Analysis*, 130, 261–274.

Hornik, K., Stinchcombe, M., and White, H. (1989), “Multilayer feedforward networks are universal approximators,” *Neural networks*, 2(5), 359–366.

Hu, L., Ji, J., and Li, F. (2021), “Estimating heterogeneous survival treatment effect in observational data using machine learning,” *Statistics in medicine*, 40(21), 4691–4713.

Jackson, C. (2016), “flexsurv: A Platform for Parametric Survival Modeling in R,” *Journal of Statistical Software*, 70(8), 1–33.

Jordan, M. I., and Jacobs, R. A. (1994), “Hierarchical mixtures of experts and the EM algorithm,” *Neural computation*, 6(2), 181–214.

Kuk, A. Y., and Chen, C.-H. (1992), “A mixture model combining logistic regression with proportional hazards regression,” *Biometrika*, 79(3), 531–541.

Künzel, S. R., Sekhon, J. S., Bickel, P. J., and Yu, B. (2019), “Metalearners for estimating heterogeneous treatment effects using machine learning,” *Proceedings of the National Academy of Sciences*, 116(10), 4156–4165.

Kuo, L., and Peng, F. (2000), “A Mixture-Model Approach to the Analysis of Survival Data,” *Generalized Linear Models: A Bayesian Perspective*, p. 255.

Lasse Hjort Jakobsen (2023), *cuRe: Parametric Cure Model Estimation*. R package version 1.1.1.

Lee, C. Y., Wong, K. Y., and Bandyopadhyay, D. (2024), “Partly linear single-index cure models with a nonparametric incidence link function,” *Statistical methods in medical research*, 33(3), 498–514.

Li, Y., Tiwari, R. C., and Guha, S. (2007), “Mixture cure survival models with dependent censoring,” *Journal of the Royal Statistical Society Series B: Statistical Methodology*, 69(3), 285–306.

Liu, Y., Kairalla, J. A., and Renfro, L. A. (2022), “Bayesian adaptive trial design for a continuous biomarker with possibly nonlinear or nonmonotone prognostic or predictive effects,” *Biometrics*, 78(4), 1441–1453.

Othus, M., Barlogie, B., LeBlanc, M. L., and Crowley, J. J. (2012), “Cure models as a useful statistical tool for analyzing survival,” *Clinical Cancer Research*, 18(14), 3731–3736.

Pan, C., Cai, B., and Sui, X. (2024), “A Bayesian proportional hazards mixture cure model for interval-censored data,” *Lifetime Data Analysis*, 30(2), 327–344.

Patilea, V., and Van Keilegom, I. (2020), “A general approach for cure models in survival analysis,” *The Annals of Statistics*, 48(4), 2323–2346.

Peng, Y., and Dear, K. B. (2000), “A nonparametric mixture model for cure rate estimation,” *Biometrics*, 56(1), 237–243.

Peng, Y., and Taylor, J. M. (2011), “Mixture cure model with random effects for the analysis of a multi-center tonsil cancer study,” *Statistics in medicine*, 30(3), 211–223.

Powers, S., Qian, J., Jung, K., Schuler, A., Shah, N. H., Hastie, T., and Tibshirani, R. (2018), “Some methods for heterogeneous treatment effect estimation in high dimensions,” *Statistics in medicine*, 37(11), 1767–1787.

Royston, P., and Parmar, M. K. (2013), “Restricted mean survival time: an alternative to the hazard ratio for the design and analysis of randomized trials with a time-to-event outcome,” *BMC medical research methodology*, 13, 1–15.

Semenova, V., and Chernozhukov, V. (2021), “Debiased machine learning of conditional average treatment effects and other causal functions,” *The Econometrics Journal*, 24(2), 264–289.

Sy, J. P., and Taylor, J. M. (2000), “Estimation in a Cox proportional hazards cure model,” *Biometrics*, 56(1), 227–236.

Tian, L., Zhao, L., and Wei, L.-J. (2014), “Predicting the restricted mean event time with the subject’s baseline covariates in survival analysis,” *Biostatistics*, 15(2), 222–233.

Williams, G., Huang, J. Z., Chen, X., Wang, Q., and Xiao, L. (2020), *wskm: Weighted k-Means Clustering*. R package version 1.4.40.

Winter, S. S., Dunsmore, K. P., Devidas, M., Wood, B. L., Esiashvili, N., Chen, Z., Eisenberg, N., Briegel, N., Hayashi, R. J., Gastier-Foster, J. M. et al. (2018), “Improved survival for children and young adults with T-lineage acute lymphoblastic leukemia: results from the Children’s Oncology Group AALL0434 methotrexate randomization,” *Journal of Clinical Oncology*, 36(29), 2926–2934.

Wu, Y., Kolassa, J., and Dong, N. (2025), “Restricted mean survival time based on Wu-Kolassa estimator compared to Kaplan-Meier estimator,” *Contemporary Clinical Trials*, 152, 107877.

Xu, S., Cobzaru, R., Finkelstein, S. N., Welsch, R. E., Ng, K., and Shahn, Z. (2024), “Estimating Heterogeneous Treatment Effects on Survival Outcomes Using Counterfactual Censoring Unbiased Transformations,” *arXiv preprint arXiv:2401.11263*, .

Xu, S. G., and Reich, B. J. (2023), “Bayesian nonparametric quantile process regression and estimation of marginal quantile effects,” *Biometrics*, 79(1), 151–164.

Zhang, J., and Peng, Y. (2007), “A new estimation method for the semiparametric accelerated failure time mixture cure model,” *Statistics in medicine*, 26(16), 3157–3171.